國 立 交 通 大 學

電控工程研究所

碩士論文

無線感測網路錨節點之反向定位法

An Approach to Reversely Locating Anchor Nodes in Wireless Sensor Network

研 究 生：李勇叡

Student: Yung-Jui Lee

指導教授：黃育綸 博士

Advisor: Dr. Yu-Lun Huang

中華民國 一百零一 年 四 月

4, 2012

無線感測網路錨節點之反向定位法

An Approach to Reversely Locating Anchor Nodes in Wireless Sensor Network

研 究 生：李勇叡　　Student: Yung-Jui Lee

指導教授：黃育綸　博士　　Advisor: Dr. Yu-Lun Huang

國 立 交 通 大 學

電控工程研究所

碩士論文

A Thesis

Submitted to Institute of Electrical Control Engineering

College of Electrical Engineering

National Chiao Tung University

in partial Fulfill of the Requirements

for the Degree of

Master

in

Institute of Electrical Control Engineering

4, 2012

Hsinchu, Taiwan, Republic of China

中華民國 一百零一 年 四 月

無線感測網路錨節點之反向定位法

學生：李勇叡　　指導教授：黃育綸　博士

國 立 交 通 大 學 電控工程研究所（研究所）碩士班

摘　　要

無線感測網路定位已經成為各種新穎應用（如土石流偵測、精緻農業、健康照護等）高度需求的功能之一。 透過錨節點（anchor node）的參考位置值及與感測節點（sensor node）之間的訊號強度，即可定位無線感測網路中的感測節點。 在這類設計中，錨節點的位置愈精確，感測節點的定位結果就會愈正確。 為了要提供精確的錨節點位置資訊，許多研究利用 GPS 裝置來定位戶外的無線感測網路中的感測節點。 由於 GPS 裝置無法在室內環境中得到精確的位置資訊，因此，有部分定位方法會利用手動設定錨節點位置的方式來得到較精確的感測節點位置。然而，手動設定錨節點的方法卻無法應用於大型無線感測網路中，而且，手動設定的人工錯誤也可能會逐漸累積，並影響無線感測網路的定位結果。 在這篇論文中，我們研究多種反向定位802.11無線網路存取點的方法。有些方法仍舊採用GPS模組來定位錨節點（存取點）的位置；有一些則嚴格地限制訓練階段的條件（固定的啓始點與行進方向）。 為了改善這些問題與限制，我們提出一種新的無線感測網路反向定位錨節點的方法。我們的方法不需要GPS模組，也不需要嚴格的訓練限制。 考慮到無線通訊晶片的個體差異，在我們開始進入訓練階段之前，我們先對無線感測節點進行校正，以取得評估節點距離所需的 RSSI 係數，以利反向定位錨節點。 我們利用 MSP430FS5438/CC2500EMK 實驗板進行多種實驗，以便於精確性與成本之間取得平衡。 我們同時也說明如何應用我們的方法來估測錨節點位置，並將估測的位置應用於現有的定位方法中，以利定位感測節點。 實驗結果顯示：1) 如果先進行校正或移除訓練限制，我們就可以得到較高的精確度; 2) 比起真正的錨節點位置，我們所估測的錨節點位置會引入大約 9.25% 的定位誤差。

An Approach to Reversely Locating Anchor Nodes in Wireless Sensor Network

Student: Yung-Jui Lee Advisor: Dr. Yu-Lun Huang

Institute of Electrical Control Engineering

National Chiao Tung University

Abstract

Wireless sensor network (WSN) localization is demanded in many modern applications, like landslide detection, precision agriculture, health care, etc. By leveraging the anchor nodes, sensor nodes in a WSN can be localized. The more precise the position of an anchor node is, the more accurate the localization of a sensor node can be. To provide the accurate positions of an anchor node, many studies have taken advantage of a GPS device placed in the outdoor environment. Since the GPS device cannot work properly in an indoor environment, some existing localization methods also adopt the configuration of the anchor node in a manual fashion. However, manually configuring anchor nodes is not suitable for large-scale WSNs and artificial errors may be propagated and thus affect the result of the WSN localization. In this paper, we study several reverse localization methods regarding locating wireless access points (AP) in an 802.11 wireless network. Some of these methods still rely on the GPS modules for AP positioning, and some others strictly restrict the training conditions. As an improvement, we propose a novel approach to locate anchor nodes in a WSN without any GPS modules or strict traninig restrictions. Considering the individual differences of wireless chips, we apply the calibration before reversely locating the anchor nodes to obtain the RSSI (received signal strength indicator) coefficients for estimating the distance between two nodes. We conduct a series of

experiments with MSP430FS5438/CC2500EMK devices to study the tradeoff between the accuracy and running cost. We also demonstrate how the proposed approach estimates the anchor nodes and applies the estimation to an existing localization method. The result shows that 1) better accuracy can be obtained if we apply the calibration or remove the training restrictions; 2) there is a gap of 9.25% errors in average between the real and estimated anchor positions.

誌謝

能夠完成此篇論文，首先要感謝我的指導教授，黃育綸博士，在我於交大的這兩年期間認真的教導我，尤其是培養我對於研究上所需要的思維， 每當我在研究上出現瓶頸時，老師總是不厭其煩的和我一起面對問題，把我導回到正確的方向，讓我保持對研究的熱忱，並且指導我正確的研究方法。 另外感謝口試委員謝續平教授、胡竹生教授以及陳右穎副教授，給予論文上的寶貴建議，使我的論文更加的完整。

感謝陳柏廷學長與實驗室同學們在口試上給予相當精闢的見解以及幫助，使我口試報告的內容更加的流暢。也感謝RTES實驗室的學長姐們、同學們以及學弟妹們，謝謝你們在這兩年的陪伴，豐富了我的研究生活，令我的研究生活增添不少的歡樂。特別感謝我的家人，當初包容我到交大唸書的決定，以及一直一來默默的支持使我能夠順利完成學業。最後也期許自己未來能夠更加的精進，有著更好的表現。

Contents

List of Figures

List of Tables

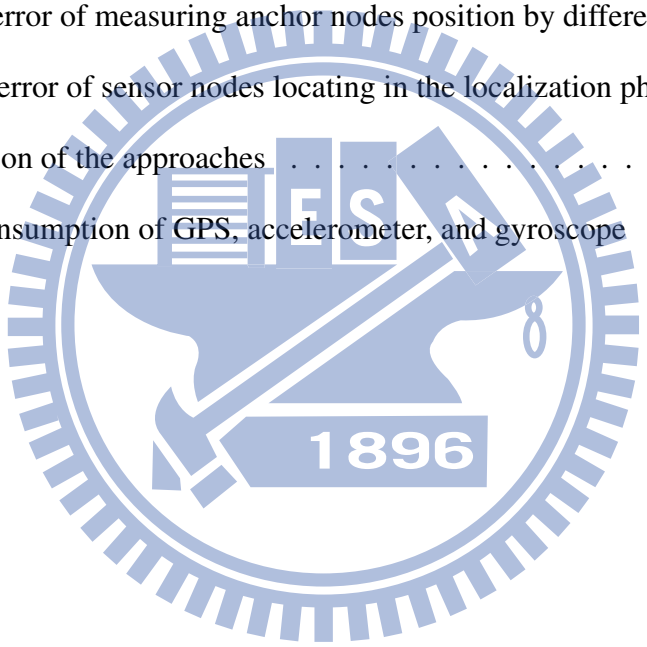

Chapter 1

Introduction

In this chapter, we first introduce the wireless sensor network. Then the requirement of the anchor node positions is discussed after. Contributions and the synopsis of this paper are mentioned in the end of this chapter.

1.1 Wireless Sensor Network

Modern wireless communication and MEMS IC technology have enabled the development of low-cost, low-power and multi-functional sensor nodes. A WSN is a network contains large numbers of such sensors and can be applied to monitoring and controlling homes, buildings, cities, rivers, forest, etc [1][2]. Self-localization capability is a highly demanded characteristic of wireless sensor network, especially in cases that sensor nodes are deployed randomly or moved after deployment. In the applications like forest fire detection, landslide detection, and precision agriculture, the sensing data are meaningless without knowing the location from where the data are obtained. Since positions of sensor nodes are subject to change, each node is equipped with a localization system, such as GPS (Global Positioning System), to report its location. However, GPS is impractical and unsuitable for WSNs due to the implementation cost and energy consumption. Moreover, the existing GPS devices are not able to provide precise locations for indoor applications. Hence, the WSN often work with different localization technologies to estimate the positions of sensor nodes.

The exists localization algorithms for sensor network usually estimate the positions of sen-

sor nodes by referring the special sensor nodes with known positions, or by measuring distances of neighboring sensors. Sensor nodes with known positions are called *anchor nodes*. The positions of anchor nodes are determined by a GPS device or set manually by the developer or administrator. The anchor nodes define the local coordinate system to which all other sensor nodes are referred. Hence, the sensor nodes, also called *non-anchor nodes*, with unknown location information can be located with different localization techniques.

In the context of the existence of *anchor nodes* (nodes with known positions), the localization algorithms can be classified into two groups: *anchor-free* and *anchor-based* algorithms [3]. Anchor-free algorithms use local distance information to attempt to determine the node coordinates [4]. Anchor-based algorithms rely on the positions of anchor nodes to precisely estimate the positions of sensor nodes. As mentioned, leveraging GPS devides [5][6][7] or manually configure the positions of anchor nodes provides referencing coordinates for an anchor-based localization algorithm. But GPS devices fail to offer precision in an indoor environment. Manual configuration is a tedious and error-prone process that is unsuitable for large-scale sensor networks. In the past few years, a number of localization algorithms have been proposed to estimate locations of wireless sensor nodes without GPS devices [8][9][10]. However, these algorithms requires more power consumption and fail to provide accurate locations of sensor nodes.

1.2 Contribution

In this research, we present an approach to reversely locate anchor nodes for anchor-based localization algorithms. Our approach automatically measures anchor positions without manual setting. With the proposed approach, the WSN applications requiring location information could facilitate with an anchor-based localization algorithm without GPS devices to locate the

anchor nodes in a WSN.

To validate the proposed approach, we design several experiments to locate sensor nodes after obtaining the anchor positions measured by our approach. We compared the performance on sensor locating in the proposed approach and other methods that locate sensor nodes by actual anchor positions. We also compare our approach with other method in terms of power consumption, extra hardware usages and the restrictions.

1.3 Synopsis

The thesis is organized as follows. We review the background of the localization system and the approaches involved to locate anchor nodes in Chapter 2. We introduce the exist approaches of finding positions of anchor nodes in Chapter 3. In Chapter 4, we explain the proposed approach of locating anchor nodes in WSN. We conduct experiments to verify the calibration algorithm in the proposed approach in Chapter 5 and demonstrate the reversely locating approach with simulation in Chapter 6. Finally, we conclude the thesis in Chapter 7.

Chapter 2

Background

In this chapter, we describe the background of our approach. We first review the RSSI-based distance estimation techniques, anchor-based localization algorithms, and explain the navigation and analysis techniques used in the proposed approach.

2.1 RSSI-based Distance Estimation

Distances or angles between two wireless nodes can be estimated by four common methods. Some of them estimate the angle between two nodes, some estimate the distances. The AoA (angle of arrival) method evaluates the relative angles between nodes by special antenna [11]. The advantage of the AoA method is the high accuracy and the disadvantage is the additional hardware. The ToA (time of arrival) and TDoA (time difference of arrival) methods estimate distances between two nodes using time based measurements. The distance is proportional to the time of the signal propagation. The methods need specific hardware and high precisely synchronized nodes. Therefore, the cost is generally high.

Based on the physical fact of wireless communication that the signal strength is inversely proportional to the distance, the RSSI (Receive Signal Strength Indicator) based method provides a feasible way to estimate distance between a transmitter and a receiver. Since no extra hardware is required for distance estimation, the RSSI-based method are the most popular localization techniques. However, the drawback of RSSI comes from the instability and susceptible environmental interference.

The instability of the RSSI-based distance estimation is resulted from the node inconsistency, where the same RSSI value represents different distance for different nodes. In Lau's study [12], the node consistency can be calibrated by assigning a propagation coefficient for each node. In Fang's study [13], the experiment result shows that the node inconsistency is greater in the receiving power than transmitting power, where the standard deviation in the transmitting power is 0.93 dBm as in the receiving power is 2 dBm. And they concluded that the requirement of calibration is only on the receiving power by adjusting the raw RSSI value by an offset value of RSSI measurement for each node.

The Log Distance Path Loss Model [14] is commonly used in the RSSI-based distance estimation:

$$PL(d) = PL(d_0) + 10n \log_{10} \frac{d}{d_0} + X_\sigma, \tag{2.1}$$

where $PL(d)$ is the path loss at distance d, d is the distance between transmitter and receiver, d_0 is the reference distance, n is the propagation constant and X_σ is a zero-mean random variable with standard deviation σ. The model provide a way to estimate path loss as a function of distance between nodes. The coefficient n defines the decrease rate of the signal strength when the distance increase.

To simplify the above function, Chipcon [15] specifies the following equation:

$$RSSI = -(10n \log_{10}(d) + A),$$

where the definitions of n and d are as the same as in Equation 2.1, and A is the received signal strength at 1 meter. Chipcon set the reference distance d_0 in Equation 2.1 to 1 meter and set $PL(d_0)$ to A as the reference signal strength constant. This provide a way to estimate RSSI value as a function between nodes.

In Zickler's study [16], a probabilistic model of RSSI-based distance estimation is proposed. The likelihood function is defined as $L(dist|rssi) = D_{rssi}(dist)$, where the probability

distribution is modeled as

$$D_{rssi}(dist) = \frac{\max(0, \sigma - \max(0, |dist - \mu| - \tau))}{\sigma},$$

where $dist$ is the distance, μ is the mean of the distribution, τ is the radius of the trapezoid's uniform center component, and σ is the radius of the trapezoid's linear falloff component. Zickler's model provide a way to estimate the probability of a receiving node at a particular distance from the transmitter as a function of the given RSSI value.

2.2 Anchor-based Localization Algorithms

Anchor-based localization algorithms usually work with RSSI-based distance estimation, since the location computing is based on the distances between anchor nodes and sensor nodes. Trilateration (or multilateration), a fundamental algorithm that can be applied to calculate position of a sensor node. To estimate position using trilateration, a sensor node needs to know the positions of three anchor nodes and its distance from each of these anchor nodes. Distances can be estimated using RSSI-based distance estimation we discussed in the previous section. The position of sensor node is computed via the intersection of three circles, as shown in Figure 2.1. The circles are represented by the formula $(x - x_i)^2 + (y - y_i)^2 = d_i^2$, where (x, y) is the po-

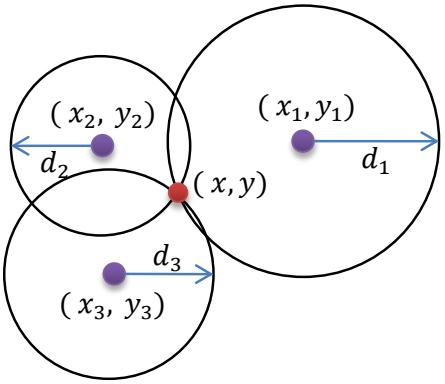

Figure 2.1: Trilateration algorithm

sition of sensor node, (x_i, y_i) is the position of the ith anchor node, and d_i is the distance from the ith anchor node to the sensor node. Furthermore, if more than three anchor nodes are available, it becomes to a overdetermined system. The overdetermined system usually has more than one solution. Gradient descent can be applied to obtain the positions of the non-anchor node achieving the least square error.

Other algorithms like bounding box [17] and probabilistic approach [18] can also use to compute node positions in anchor-based algorithms. The bounding box algorithm uses squares instead of circles (in trilateration algorithm) to bound the possible position of a sensor node. The probabilistic approach algorithm models the errors in distance estimation between anchor nodes and sensor nodes as normal random variables for calculating the probable position of a sensor node. However, due to the computing complexity, the trilateration algorithm is more popular to be applied in WSN.

Due to the power consumption and localization accuracy, the anchor-based algorithms are the most popular localization algorithms in WSN. The anchor-based algorithms locate sensor nodes under the assumption of the precise position of anchor nodes. If the position of anchor nodes are configured inaccurately, the incremented error may seriously influence on the sensor locating accuracy. Hence, the precise anchor node position is the main requirement of anchor-based algorithms.

2.3 Inertial Navigation System

Inertial navigation, a self-contained navigation technique, adopts accelerometers and gyroscopes to track the position and orientation of an object relative to a known starting point, orientation and velocity [19]. Inertial Measurement Units (IMUs) typically use three orthog-

onal gyroscopes and three orthogonal accelerometers to measure angular velocity and linear acceleration respectively. The advances in the construction of MEMS devices in recent years have made it possible to manufacture small and light inertial navigation systems. These advances have widened the applications to include human and animal motion capture. The inertial navigation system estimates the position and orientation of a moving object by continuously tracking the output from a number of sensors in the IMUs attached to the object [20].

2.4 Procrustes Analysis

Procrustes analysis is a well-known technique to transform one set of data to represent another set of data as closely as possible [21][22]. The Procrustes analysis provides least squares matching of two or more set of data for the multidimensional rotating, translating, and uniformly scaling of different matrix configurations. It is first applied in the factor analysis, and has become a popular method of shape analysis [23]. Moreover, the Procrustes analysis is applied to coordinate transformation [24]. Specifically, given a set of reference coordinates, X, and a set of coordinates to be transformed, Y. Procrustes gives a transformation that minimizes the difference between X and the transformed coordinates, Z, as in the equation as

$$Z = s \times Y \times R + t.$$

In the equation, s is the scalar, R is the rotation/reflection, and t is the translation, each of them is determined by the Procrustes analysis to minimize the sum of squared errors between X and transformed Z.

For example, the given coordinates set $X = \{(x_1, y_1); (x_2, y_2); (x_3, y_3)\}$ and the coordinates set to be transformed $Y = \{(x'_1, y'_1); (x'_2, y'_2); (x'_3, y'_3)\}$. The Procrustes analysis gives the transformed set Z with scaling, rotating, and translating as shown in Figure 2.2.

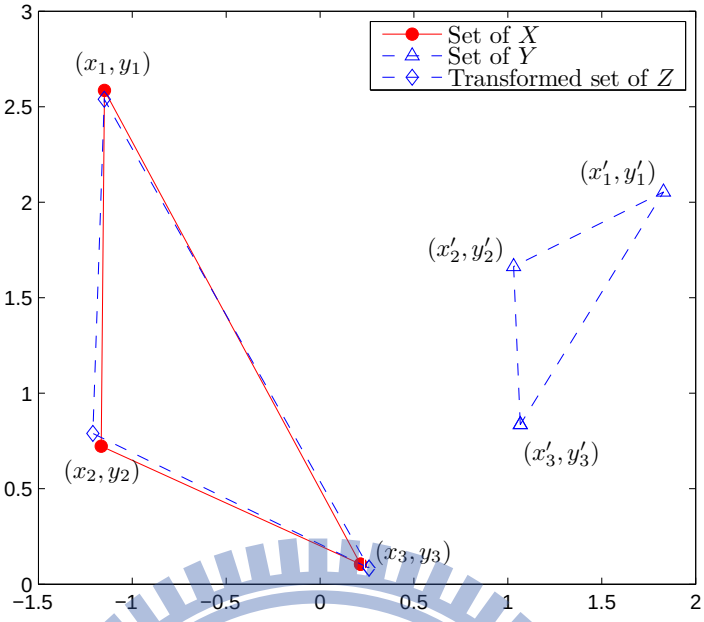

Figure 2.2: Example of Procrustes analysis

2.5 Summary

Estimating distance between nodes based on RSSI is a popular way in the WSN localization system. The problem of the RSSI-based distance estimation is the node inconsistency. It can be solved by calibrating each node for the propagation coefficient independently. Anchor-based algorithms with RSSI-based distance estimation provide higher accuracy and lower power consumption for the localization applications. The main requirement of the anchor-based algorithm is the positions of anchor nodes, where the accuracy of these positions may affect on the accuracy of sensor node locating. However, the current methods failed to provide precise positions for anchor nodes. To solve the problem, we proposed an approach, which integrated with an INS (Inertial Navigation System) and Procrustes analysis, in WSN for the application of localization.

Chapter 3

Related Work

In this chapter, we first introduce the method of reverse locating anchor nodes in WSN. We also discuss the pros and cons of existing methods of reversely locating Wi-Fi access points (APs) location and make a brief summary.

3.1 Reversely Locating Anchor Nodes

The positions of anchor nodes in WSN are usually configured by GPS device or manual setting. GPS is only suitable for outdoor environment and is an additional hardware that increases the cost and the power consumption of nodes in WSN. Manually configuring the anchor positions is a tedious procedure, which may involve artificial errors and is not suitable for a large-scale wireless sensor network. Therefore, an efficient method is required to locate anchor nodes in a WSN.

In 2008, Du [25] proposed a method to locate anchor nodes for WSN by magnetic dipoles and GPS information in outdoor environment. They assumed that anchor nodes are all equipped with magnetic dipoles and sprinkled evenly over the area. An aircraft with magnetic detection instrument and GPS receiver then scans over the area and captures the magnetic dipole moment with GPS information. Based on the magnetic dipole moment, the algorithm can obtain the distance between the anchor nodes. However, such an algorithm requires additional modules like magnetic dipole for each anchor nose. For adopting magnetic dipole, the algorithm works

well only in outdoor environments.

Most localization algorithms are designed for locating sensor nodes in a wireless sensor network. None of them emphasize the reverse localization for anchor nodes. The existing reverse localization algorithms are designed for finding Wi-Fi Access Point (AP) position in Wi-Fi network. The positions of APs can then be used in a Wi-Fi-based Localization System to locate Wi-Fi devices. Since APs in Wi-Fi network are similar to anchor nodes in WSN, algorithms of finding AP positions can also used to locate anchor nodes in a WSN.

For indoor environments, Ekahau HeatMapper is a free tool to find Access Points (APs) in Wi-Fi networks. HeatMapper is a good and free way to map APs in small Wi-Fi networks, and the positions of APs are relatively accurate. However, it is not supported in the network with other wireless protocols, like Zigbee and Bluetooth. After importing a floor plan image as a map, a user carrying the laptop with HeatMapper installed walks slowly around the floor and manually records the location of user on the map frequently. HeatMapper constantly collects signal data from APs when the user walks around. Then, HeatMapper combines the signal data, calculates and displays the locations of AP on the map. Figure 3.1 is a screen shot of the Ekahau HeatMapper downloaded from www.ekahau.com. Six APs are found along with the walking route. Figure 3.2 shows the real test of Ekahau HeatMapper in the second floor, Engineering Building 5, Kuang-Fu campus of National Chiao Tung University. We can see that the positions of Wi-Fi APs named EE207, EE208, and EE209 (deployed in room 207, 208, and 209), as noted on the figure, are relatively accurate. But there still many Wi-Fi APs are not localized by Ekahau HeatMapper. The disadvantage of the HeatMapper is the requirement of floor plan. Without the floor plan, the positions are manually recorded with huge errors. Also, the artificial error are included with the manual recording. Nevertheless, the method is still worth for reference.

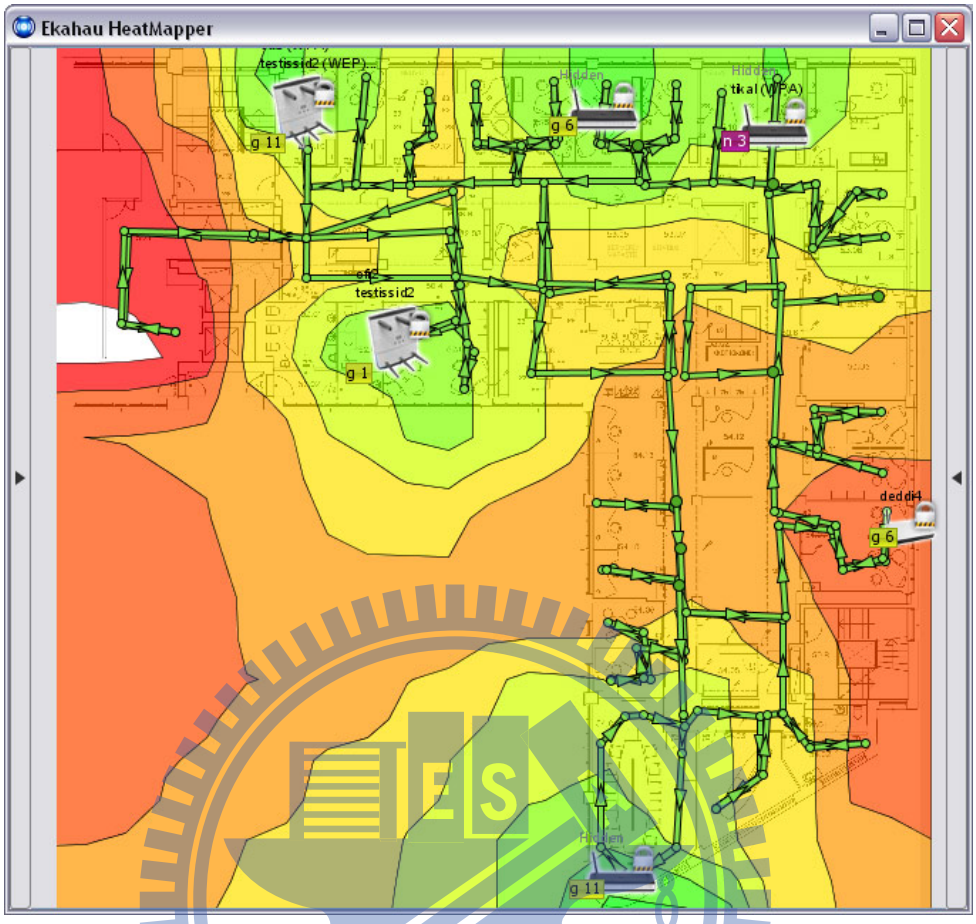

Figure 3.1: A screen shot of Ekahau HeatMapper (Source: www.ekahau.com)

3.2 Jones' Method

In 2008, Jones [26] has developed a method to reversely locate Wi-Fi APs by a special vehicle. The vehicle is equipped with an AP scanning device, a GPS device, a Wi-Fi radio device and a Wi-Fi antenna system. The steps of the method is described as below:

1. The vehicle moves in a programmatic route.

2. The vehicle scans for Wi-Fi APs and collects RSSI values from the scanned APs.

3. The vehicle obtains the GPS coordinates through th GPS receiver.

4. The vehicle sends the collected RSSI and GPS coordinates to a control server (named "Central Network Server" in the paper).

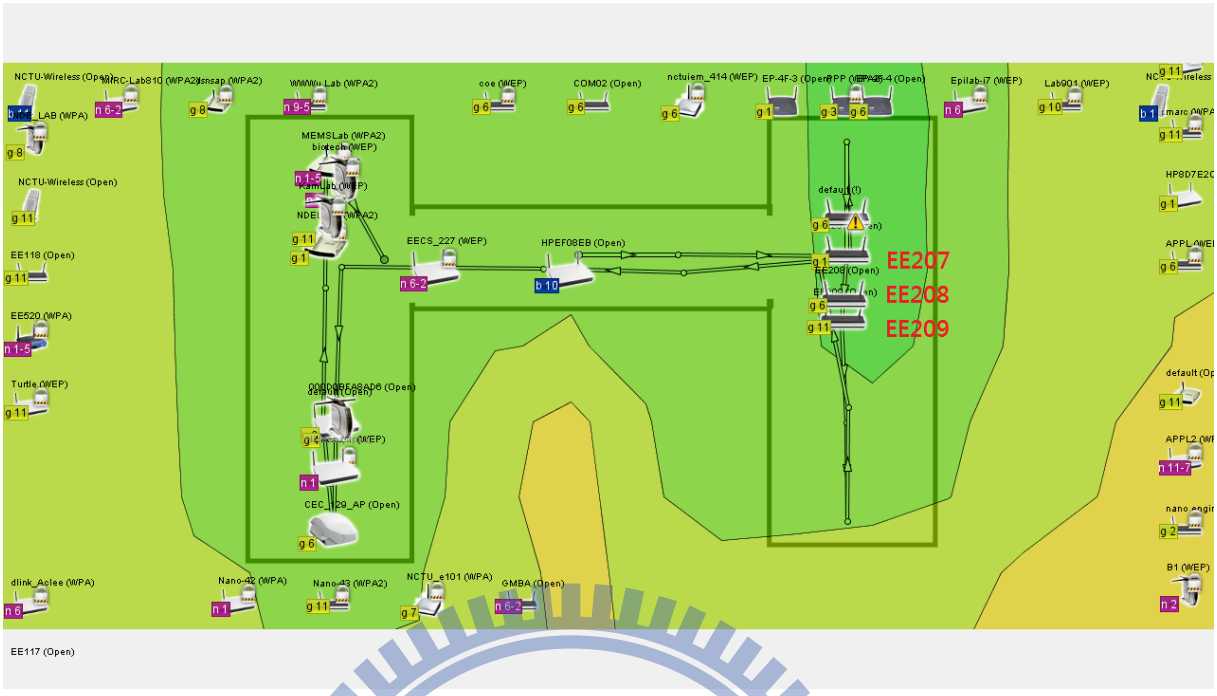

Figure 3.2: The testing result of HearMapper

5. The server computes AP locations with the reverse trinagulation algorithm.

However, such a special vehicle is expensive and is restricted to move on a smooth or flat plane. In addition, the GPS device cannot provide precise coordinates when working in indoor environment.

3.3 Chun's Method

In 2011, Chun *et al.* [27] inten to reversely locate APs by leveraging the GPS module in a smartphone. They assumed that the smartphones, equipped with GPS modules, can receive GPS signal both indoor and outdoor. Also, the smartphone can access Internet through Wi-Fi networks. The method involves 5 steps:

1. Place more than one smartphones are placed at different positions in an area.

2. The smartphones scan and collect RSSI values from the nearby APs.

3. The smartphones obtain GPS coordinates.

4. The smartphones upload the vector $< x, y, r, AP\_MAC\_ID >$ to a control server, such that the server can store the vector in the database. The parameters of x and y are the x-axis and y-axis of the coordinates obtained from GPS and r is the RSSI value from AP with the MAC identifier AP_MAC_ID.

5. The control server computes AP locations by Chun's heuristic solution.

In their simulation, only one AP has been placed in the simulation area of 400 m $\times$ 300 m. The coverage range of the AP is set to 100 meters. Assuming that the RSSI distortion is 20%, if 6 smartphones are used, the distance error ranges from 2m to 32m. The distance error reduces to 1m 9m if 15 smartphones are used. Their experiments shown an average distance error of 3.46 meter. The method overcomes the cost and unavailability of a customized vehicle, but suffers from low accuracy when locating indoor APs.

3.4 Hansson's Method

To solve the inaccuracy problem resulted from bad indoor GPS signals, in 2011, Hansson and Tufvesson [20] have developed a method to reversely locate Wi-Fi AP by obtaining sensing data from gyroscope, accelerometer, and magnetometer. First, an inertial navigation system (INS) is developed on a smartphone with accelerometer, gyroscope, and magnetometer. The INS is composed of an orientation tracker and a step detector and is used to record the walking path of a user. Assume that the start position and orientation are known and fixed, the navigation system can locate the AP with a global coordinates. In Hansson's method, the error model of the navigation system is presented with a linear functin of two variables $e(t, d)$, where t is the navigation time (in seconds) and d is the estimated distance (in meters). The coefficients of the

error model are defined as

$$e(t, d) = -0.2398 + 0.0152t + 0.1081d, \tag{3.1}$$

where e is the estimated error in meters. Hansson's method is described as below:

1. A user carries a smartphone and walks around the testing area.

2. The smartphone continuously scans the Wi-Fi environment and determines the RSSI values for all nearby APs.

3. For each RSSI attained, the smartphone record the position by the navigation system.

4. The smartphone generates a vector $\mathbf{m}_k = < AP\_MAC\_ID, r, x, y, e >$, where x and y are the coordinates and e is the estimated error of the position and r is the measured RSSI value from AP with MAC identifier AP_MAC_ID. Then, the smartphone uploads the vector to the control server.

5. The control server computes AP locations with the trilateration algorithm.

The overall system is shown in Figure 3.3. In their experiments, 6 APs are placed in a 60m $\times$ 40m test field 18 walks are conducted. The results show that the position error of measured AP positions and actual AP positions is from 0m to 10m and the average position error is 4.5m.

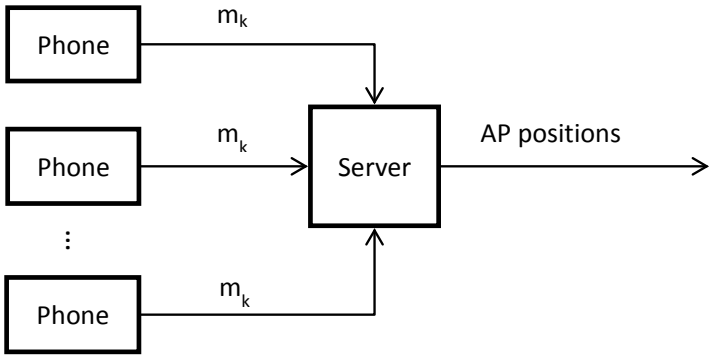

Figure 3.3: The system architecture of Hansson's method

Hansson has mentioned that the following restrictions that be fulfilled to obtain accurate results:

- **Known starting direction:** The user is required to face to a known direction (e.g. north) initially.
- **Known starting position:** The user is required to start at a known place.

With restrictions, the estimated positions of navigation system are always accurate at the start point but obtain larger errors when getting far from the starting position. Thus, the error of the located AP positions raises with the error of estimated positions of navigation system. The restrictions also come with artificial errors when selecting the starting direction and position.

3.5 Summary

We introduce the common methods locating anchor nodes in a WSN localization system. Since there are few researches in the localization of anchor nodes in WSN, we also introduce and discuss the problems of the researches of finding AP locations in a Wi-Fi network. Each of them has some drawbacks. Ekahau Heatmapper introduces artificial errors when recording the walking path and requires a floor plan. Jone's method suffers from the expensive and customized vehicle, which is not easy to implement into other systems. Chun's method suffers from the poor GPS function in indoor environments. And Hansson's method has undesirable restrictions on the starting direction and position.

Chapter 4

Proposed Approach

In this chapter, we detail the proposed approach to reversely locate anchor nodes before an anchor-based localization system is applied. Our approach estimates the anchor positions by measuring RSSI measurements of wireless signal strength. With the measured anchor positions, the existing anchor-based localization algorithms can locate moving nodes more precise. In our approach, we define four types of devices and two phases for reverse anchor localization. In this chapter, we first describe, and explain the proposed phases. In the end, we give a case study adopting the proposed approach.

4.1 Preliminaries

In addition to anchor nodes and sensor nodes, we introduce two more devices used in out approach, including training nodes and a control server.

- **Anchor nodes**, $\mathbf{A}_i$: An anchor node, normally placed at a static/fix place, is used in a localization system for localizing sensor nodes within a testing area. $\mathbf{A}_i$ represents the i^{th} anchor node, where $i = 1, 2, \cdots, I$ if maximum I anchor nodes are place in the testing area.
- **Sensor nodes**, $\mathbf{S}_j$: A sensor node, normally moving around an area and helping collect data, should be tracked by a localization system. $\mathbf{S}_j$ represents the j^{th} sensor node, where $j = 1, 2, \cdots, J$ if at most J sensor node(s) are deployed in the field.
- **Training nodes**, $\mathbf{T}_k$: In the proposed approach, some training nodes are used for re-

versely locating anchor nodes. Different from sensor nodes, a training node is assumed to be equipped with gyroscope and accelerometer and is capable of recording its roaming paths. $\mathbf{T}_k$ represents the k^{th} training node, where $k = 1, 2, \cdots, K$ if at most K training node(s) are used to reversely locate anchor nodes.

- **Control server** : The server is the center of the localization system that the all computing take place. In our approach, the server is implemented in Matlab (The MathWorks, USA) Version 7.10.0.499 (R2010a).

In our approach, we also assume that $\mathbf{A}_i$, $\mathbf{T}_k$ and $\mathbf{S}_j$ can be existed in two parallel planes with height difference h, as shown in Fig. 4.1, where three $\mathbf{A}_i$ are placed on the upper plane and a $\mathbf{T}_k$ is moving on the lower plane. The height difference h between the two planes is fixed and configured in the control server.

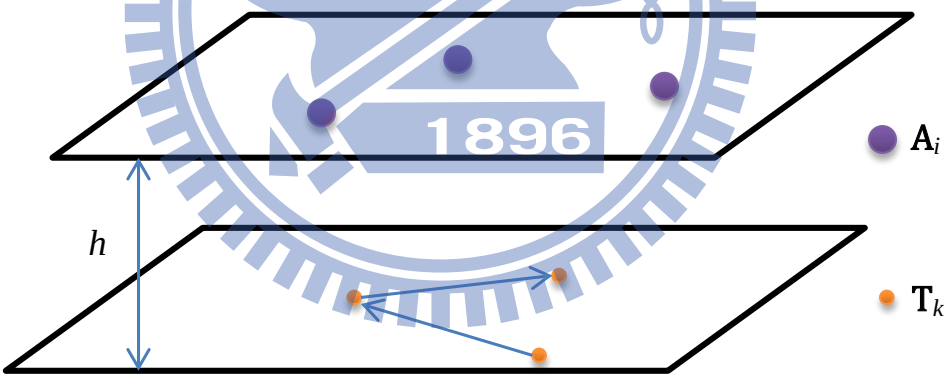

Figure 4.1: Nodes in two parallel planes

4.2 Phases

There are two phases defined in our approach: calibration and training. The calibration phase is to calibrate node inconsistency of the RSSI measurements between different nodes. The training phase is to locate anchor nodes. The followings give the details of each phase.

4.2.1 Calibration

In our approach, the distances between each node are estimated via RSSI (Received Signal Strength Indicator) values. The RSSI value is based on the physical fact of wireless communication and decreases with increased distance. Log Distance Path Loss Model [14] is a basic way of estimating path loss as a function of distance between the nodes as shown in Eq.(2.1). By revising Eq.(2.1) and replacing the initial path loss ($PL(d_0)$) with the environmental interference, we can obtain the following equation:

$$PL(d) = P + 10n \log_{10} d + X_\sigma. \tag{4.1}$$

Where d is the distance between transmitter and receiver, $PL(d)$ and is the pass loss of signal strength at distance d, P is the environmental interference, n is the path loss exponent (rate at which signal decays), and X_σ is a zero-mean Gaussian random variable with standard deviation σ. From the realistic collection of RSSI values, we found that the value of $PL(d_0)$ is not only determined by the initial path loss. It depends on the environments and nodes, so we revised it to the environment interference P and determine the value of P via the calibration process below. As receiving an input power, the distance is obtained by reversing the function in the above equation while the Gaussian noise is assumed negligible:

$$d = 10^{\frac{PL(d)-P}{10n}}.$$

And when RSSI value is adapted in, the equation is derived as:

$$d = 10^{\frac{-RSSI-P}{10n}}. \tag{4.2}$$

The previous studies on radio propagation patterns [13][28][29] show that non-isotropic path loss may come from various transmitting medium and direction in different environments. Also, there exists physical differences between each node on RSSI measurements. Therefore,

there is a need to obtain CPC (calibrating propagation coefficients) for each node and for each environment. As the study of [13], there are more requirement on calibrating for the receiving than transmitting of RSSI measurements, we only calibrate the nodes which requires to receive RSSI values: training nodes (receiving in the training phase) and anchor nodes (receiving in the localization phase).

To find the CPC for each device, we derive the Equation 4.2 as:

$$\log_{10} d = \frac{-1}{10n} \times RSSI - \frac{P}{10n}.$$

Since it becomes a linear equation, the value of n and P can be calculated by linear regression. When we set r to RSSI value, $a = \frac{-1}{10n}$, and $b = -\frac{P}{10n}$, the linear equation is derived as:

$$\log_{10} d = ar + b.$$

For the collected RSSI values,$(r_1, r_2, \cdots, r_n)$, at distances of $(d_1, d_2, \cdots, d_n)$, the matrix of the linear equation becomes:

$$Y = AX,$$

where

$$Y = \begin{bmatrix} \log_{10} d_1 \\ \log_{10} d_2 \\ \vdots \\ \log_{10} d_n \end{bmatrix}, A = \begin{bmatrix} r_1 & 1 \\ r_2 & 1 \\ \vdots & \vdots \\ r_n & 1 \end{bmatrix}, X = \begin{bmatrix} a \\ b \end{bmatrix}.$$

Then the value of a and b are obtained by the least square solution

$$X = (A^T A)^{-1} A^T Y.$$

The coefficients a and b are called the CPC (calibrated propagation coefficients) for distance estimation. And the distance between transmitter and receiver is calculated as inputting a RSSI

value to the equation:

$$d = 10^{(a \times RSSI + b)}. \tag{4.3}$$

4.2.2 Training

The objective of this phase is to locate anchor nodes and used the anchor nodes to locate sensor nodes in the localization applications. In the phase, a set of training nodes $\mathbf{T}_k$, ($k = 1, 2, \cdots, K$) and the control server are used for the purpose, as illustrated in Figure 4.2. The

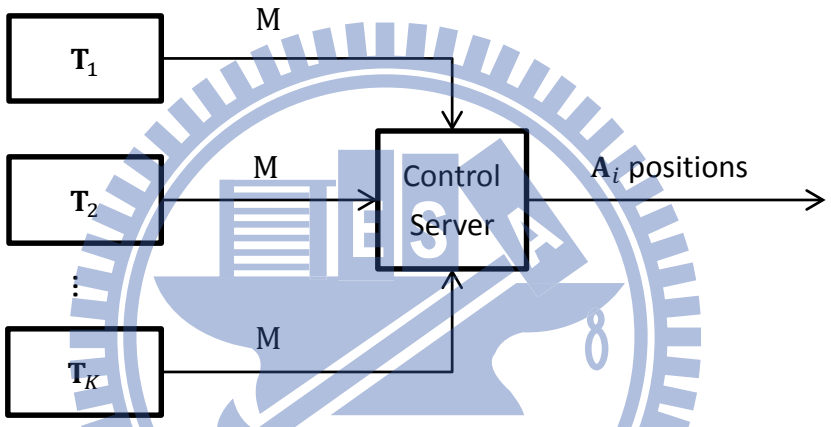

Figure 4.2: The architecture of training phase

two parts of the phase are separated, one part is running on K numbers of training nodes and the other part is running on the control server. And M is the message that $\mathbf{T}_k$ sends to the control server. The behavior of the training nodes and the server and the format of the message, M, are discussed in the following sections. Before the training phase start, there are two system parameters to be defined:

- K: the number of training nodes using for locating anchor nodes.
- **MRC**: the minumum RSSI collection for each $\mathbf{A}_i$. It defines the minimum numbers of RSSI value should be collected for an anchor node during the training of a $\mathbf{T}_k$.

Training node, $\mathbf{T}_k$

In the training phase, training nodes, $\mathbf{T}_k$, are use to collect RSSI values from the anchor nodes for locating anchor nodes. We assume that $\mathbf{T}_k$ knows the number of anchor nodes in the test plane to be located. And each $\mathbf{T}_k$ has its own local coordinate system, $\mathbb{C}_k$, and can record its own position, $\mathbb{C}_k(x, y)$, at $\mathbb{C}_k$. The position of $\mathbf{T}_k$ is recorded by a modified navigation system from Hansson's method [20]. Our modified navigation system has no restrictions on the starting direction and position, since the restrictions of fixed starting direction and position are only using for confirming all navigation systems are on the same coordinate system. The $\mathbb{C}_k$ is substituted for the same coordinate system on the $\mathbf{T}_k$. For each $\mathbf{T}_k$, the local coordinate system, $\mathbb{C}_k$, is initialized when it starts: the starting position of $\mathbf{T}_k$ is defined to be the origin of $\mathbb{C}_k$ as $\mathbb{C}_k(0, 0)$ and the starting direction of $\mathbf{T}_k$ is defined to be the positive x-axis of $\mathbb{C}_k$ as $\mathbb{C}_k(+, 0)$. Thus, for K training nodes, there are K local coordinate systems: $\mathbb{C}_1$, $\mathbb{C}_2$, $\cdots$, and $\mathbb{C}_K$. And there are relations of rotation and translation between each $\mathbb{C}_k$.

The behavior of the training nodes is illustrated in Figure 4.3. For each $\mathbf{T}_k$, it initializes $\mathbb{C}_k$ by the starting position and direction in the beginning. Then, user carries $\mathbf{T}_k$ walking around the test plane. During the walking, $\mathbf{T}_k$ continuously communicate with $\mathbf{A}_i$, which are deployed in the test plane before the $\mathbf{T}_k$ starts, and determine RSSI values for all nearby $\mathbf{A}_i$. As a RSSI value is collected, the message of

$$\mathrm{M} = (i, r, \mathbb{C}_k(x, y), e)$$

is generated and sent to the control server, where i is the identifier of anchor node, r is the measured RSSI value from $\mathbf{A}_i$, $\mathbb{C}_k(x, y)$ is the position of $\mathbf{T}_k$ in $\mathbb{C}_k$ at receiving r , and e is the estimated error of the position by the navigation system. Additionally, a variable for the numbers of collected RSSI values from $\mathbf{A}_i$ is stored in $\mathbf{T}_k$, which is noted as n_i. To notify the user when to stop the training, $\mathbf{T}_k$ examines the value of n_i every time it changes. When

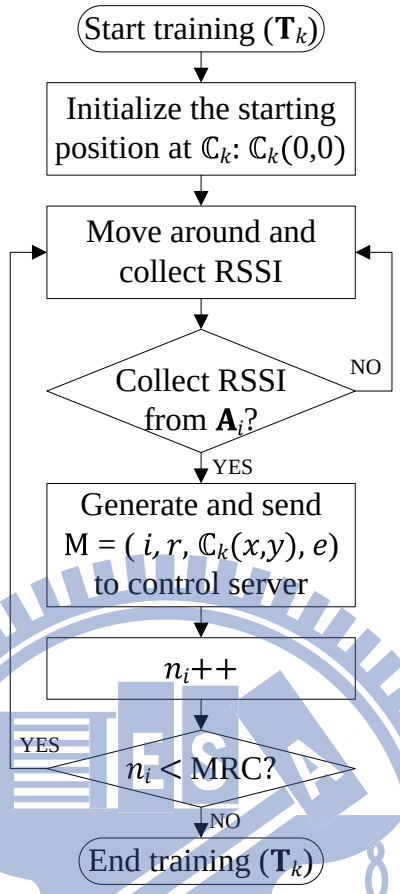

Figure 4.3: The system flow of a training node

the value of n_i for all $\mathbf{A}_i$, $i = 1, 2, \cdots, I$, are less than MRC, $\mathbf{T}_k$ notifies the user to keep walking around. The user continue walking and measuring for anchor nodes until all n_i values are greater than or equal to MRC. As the ending of a training node, it sends an end message to notice the server. And when the control server receives end messages from all $\mathbf{T}_k$, it measures the anchor positions at $\mathbb{C}_k$.

However, the measured anchor positions cannot be used in the localization application yet, since they are independent in each $\mathbb{C}_k$ and need to be integrated to a global coordinate system, $\bar{\mathbb{C}}$. In our approach, this is handled on the server by the Procrustes Analysis.

Control Server

In the training phase, the control server measures the anchor positions after the training of $\mathbf{T}_k$. The behavior of the control server can be separated into two parts: after training of each $\mathbf{T}_k$ and after training of all $\mathbf{T}_k$, as illustrated in Figure 4.4. In the first part, the control server

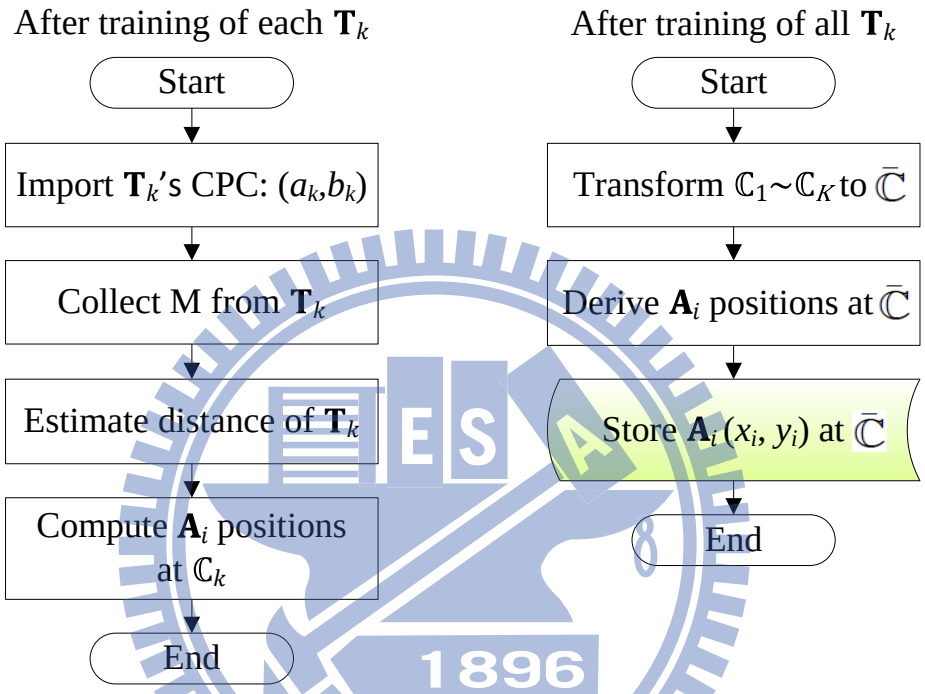

Figure 4.4: The system flow of the server

computes $\mathbf{A}_i$'s positions in each $\mathbb{C}_k$. Then in the second part, the control server transforms all $\mathbb{C}_k$ to a global coordinate system ($\bar{\mathbb{C}}$). At first, the $\mathbf{T}_k$'s CPC, obtained in the calibration phase, are imported to the control server as (a_k, b_k) for $k = 1, 2, \cdots, K$. When a training node, $\mathbf{T}_k$, ends the training and sends the end message, the control server estimates distances by the RSSI values in the message M from $\mathbf{T}_k$. The distances are estimated by

$$d = 10^{(a_k \times r + b_k)},$$

where the uploading training node is $\mathbf{T}_k$. As the training node and anchor nodes are in two parallel planes with height difference h, the distances in two planes are projected into one plane

as $\hat{d}$ by

$$\hat{d} = \sqrt{d^2 - h^2}.$$

When the distances of training node and anchor nodes on the same plane are obtained, the positions of anchor nodes are measured by trilateration algorithm. Trilateration algorithm determines the position of on object based on simultaneous distance measurements from three or more reference points at known locations. For example, considering the ideal case of measuring position of $\mathbf{A}_3$ from three uploaded vector of M from $\mathbf{T}_1$:

$$\mathrm{M}_1 = (3, r_1, \mathbb{C}_1(x_1, y_1), e_1),$$

$$\mathrm{M}_2 = (3, r_2, \mathbb{C}_1(x_2, y_2), e_2),$$

$$\mathrm{M}_3 = (3, r_3, \mathbb{C}_1(x_3, y_3), e_3).$$

The 3 circles obtained from the training node $\mathbb{C}_1(x_1, y_1)$, $\mathbb{C}_1(x_2, y_2)$, and $\mathbb{C}_1(x_3, y_3)$ and distances $\hat{d}_1$, $\hat{d}_2$, $\hat{d}_3$, will intersect at exactly on point, as shown in Figure 4.5. But in the case of

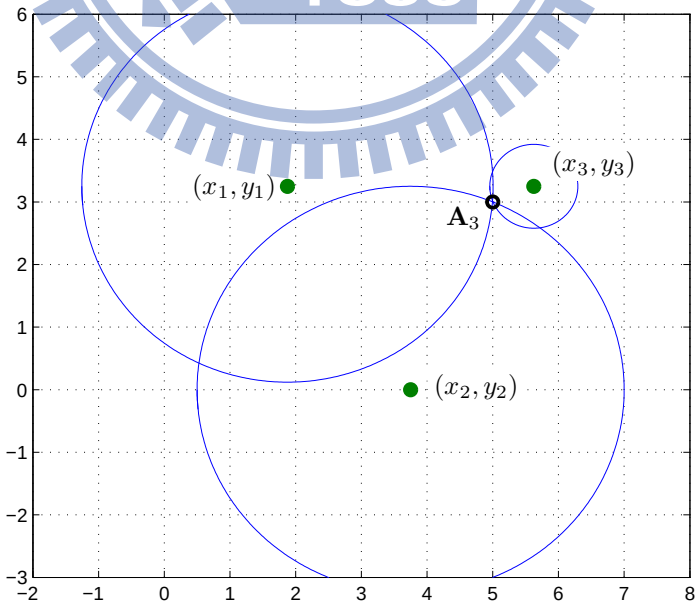

Figure 4.5: Example of trilateration in ideal case

noisy measurements, the circles may intersect in an area or not intersect at all. In such cases,

the trilateration algorithm gives the solution of the minimum error. For the measuring of anchor node $\mathbf{A}_i$, assume that N measured $\hat{d}$ at positions $\mathbb{C}_k(x, y)$, the matrices of trilateration are formed as:

$$X = \begin{bmatrix} s \\ x_i \\ y_i \end{bmatrix}, A = \begin{bmatrix} 1 & -2x_1 & -2y_1 \\ 1 & -2x_2 & -2y_2 \\ \vdots & \vdots & \vdots \\ 1 & -2x_N & -2y_N \end{bmatrix}, B = \begin{bmatrix} (\hat{d}_1)^2 - (x_1)^2 - (y_1)^2 \\ (\hat{d}_2)^2 - (x_2)^2 - (y_2)^2 \\ \vdots \\ (\hat{d}_N)^2 - (x_N)^2 - (y_N)^2 \end{bmatrix},$$

where (x_i, y_i) is the estimated position of $\mathbf{A}_i$ in the $\mathbb{C}_k$ of $\mathbf{T}_k$ and $s = {x_i}^2 + {y_i}^2$. We can write the solution of $\mathbf{A}_i$ as $X = A^{-1}B$ only if $N = 3$ and A^{-1} exists. If $N > 3$, we can solve the equation by $X = A^{+}B$, where A^{+} is the *pseudo-inverse* of A. On solving, this gives the least square error of the solution, and the $\mathbf{A}_i$'s positions at $\mathbb{C}_k$ are the estimated as $\mathbb{C}_k(x_i, y_i)$.

The second part starts after the end of training for all $\mathbf{T}_k$, the control server derives the global coordinate system ($\bar{\mathbb{C}}$) and transforms K sets of $\mathbf{A}_i$'s positions at $\mathbb{C}_k(x_i, y_i)$ into $\bar{\mathbb{C}}$. To transform these sets to $\bar{\mathbb{C}}$, the Procrustes Analysis (PA) [22][30][31] is introduced to our approach. PA is a well-known method to provide the least square matching of two matrices, where the relation between two matrices is a linear transformation of translation, reflection, orthogonal rotation, and scaling as we discussed in Chapter 2.4. In our approach, we assume that the relative measured positions of $\mathbf{A}_i$ at $\mathbb{C}_k$ are similar. Thus, we can integrate K sets of $\mathbb{C}_k(x_i, y_i)$ to $\bar{\mathbb{C}}$ base on the measured anchor positions of $\mathbf{A}_i$. First, the $\mathbf{A}_i$'s positions at $\mathbb{C}_k$ are noted as Y_k and Z_k is the transformed set of $\mathbf{A}_i$'s positions at $\bar{\mathbb{C}}$ from $\mathbb{C}_k$. The $\mathbb{C}_1$ is set as the $\bar{\mathbb{C}}$, which means $Z_1 = Y_1$, and $\mathbb{C}_k$ ($k = 2, 3, \cdots, K$) are transformed to $\bar{\mathbb{C}}$. Since the relations between each $\mathbb{C}_k$ are translation and rotation, the scalar factor is not involved in our approach. Hence, the equation of the PA is modified as

$$Z_k = Y_k \times R + t,$$

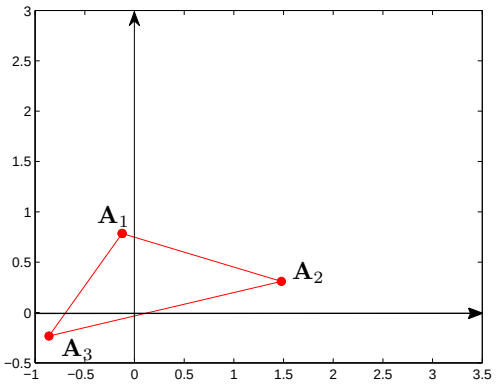

Figure 4.6: Y_1 ($\mathbf{A}_i$ positions at $\mathbb{C}_1$)

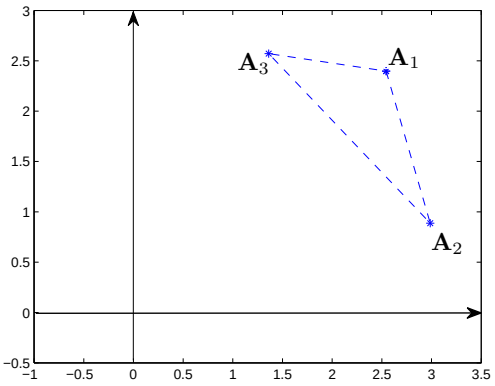

Figure 4.7: Y_2 ($\mathbf{A}_i$ positions at $\mathbb{C}_2$)

where R and t are the rotation matrix and translation matrix respectively. The Procrustes analysis gives the Z_k that

$$\min_{R,t} E = Z_k - Z_1.$$

And after all Z_k ($k = 2, 3, \cdots, K$) are obtained, the average of Z_k are the $\mathbf{A}_i$ positions, and are stored on the control server for the use of locating sensor nodes in the localization applications. For example, three anchor nodes ($\mathbf{A}_1, \mathbf{A}_2, \mathbf{A}_3$) are located by two training nodes ($\mathbf{T}_1, \mathbf{T}_2$). The measured $\mathbf{A}_i$ positions Y_1 ($\mathbf{A}_i$ positions at $\mathbb{C}_1$) and Y_2 ($\mathbf{A}_i$ positions at $\mathbb{C}_2$) are shown in Figure 4.6 and Figure 4.7. Since $\bar{\mathbb{C}} = \mathbb{C}_1$ and $Z_1 = Y_1$, the Y_2 is transformed to $\bar{\mathbb{C}}$ as Z_2, which is shown in Figure 4.8.

4.3 Proposed Approach

In Chapter 4.2, we've defined the two phases in our proposed approach. This section provides an overview of how the different phases work together in proposed system. The architecture is shown in Figure 4.9, two phases of calibration and training organize the complete system and three types of data to be stored on the control server: $\mathbf{T}_k$'s CPC, $\mathbf{A}_i$'s CPC and $\mathbf{A}_i$ positions. After our proposed system is the localization applications, which locate $\mathbf{S}_j$ with the

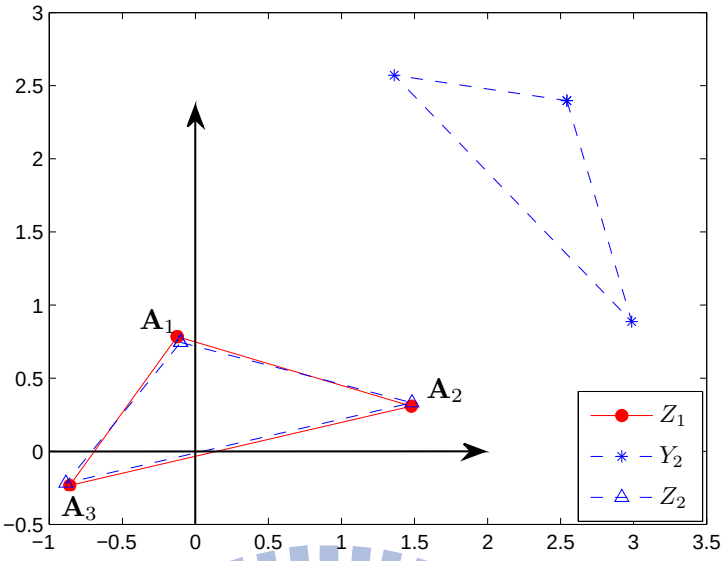

Figure 4.8: The example of transform Y_2 from $\mathbb{C}_2$ to $\bar{\mathbb{C}}$

$\mathbf{A}_i$ positions and $\mathbf{A}_i$'s CPC we supplied. The calibration phase is executed first, which outputs

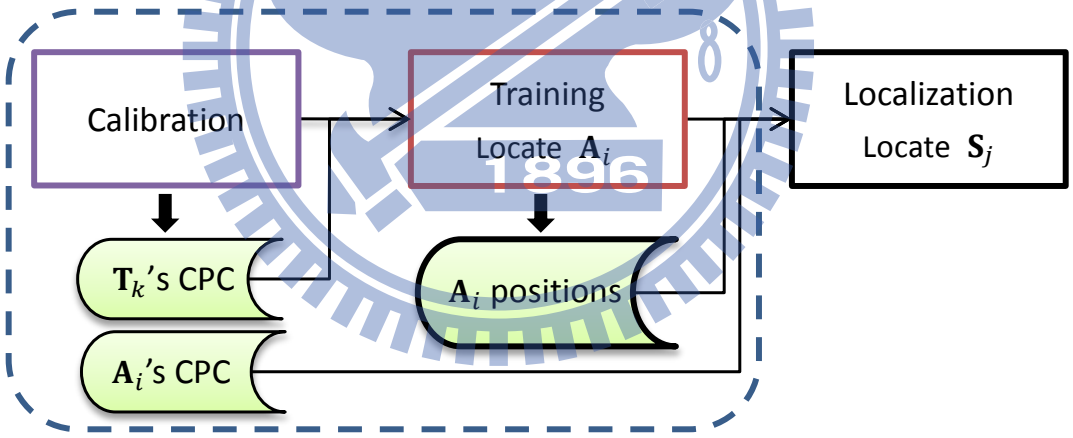

Figure 4.9: The proposed approach with two phases

the $\mathbf{T}_k$'s CPC and $\mathbf{A}_i$'s CPC and stores them on the control server. The $\mathbf{S}_j$ are not calibrated cause of the characteristic large numbers of sensor nodes in WSN and the roles of transmitting node. The number of $\mathbf{T}_k$ and $\mathbf{A}_i$ are relative lower than $\mathbf{S}_j$ and each of them is acting as the receiving node in the training phase and localization applications. Thus, for the efficiency, we only calibrate for $\mathbf{T}_k$ and $\mathbf{A}_i$.

After the calibration phase is the training phase, which outputs the measured $\mathbf{A}_i$ positions

and stores them on the control server. In the training phase, there are two parameters to be defined: K (used $\mathbf{T}_k$ numbers)and MRC (threshold of collected RSSI values). These two parameters affect the precision of measured $\mathbf{A}_i$ positions and the cost of the proposed approach. Theoretically, the larger K, the more accurate at measured $\mathbf{A}_i$ positions, but the more cost due to more devices of $\mathbf{T}_k$ are used. Similarly, the larger MRC, the more accurate at measured $\mathbf{A}_i$ positions, but the longer duration of the training due to more RSSI values to be collected from an $\mathbf{A}_i$. Therefore, there is a need to decide the number of K and MRC for the appropriate settings. For that, two experiments are designed to determine the appropriate number of the two parameters for balancing the accuracy and the cost of time and funding.

As the $\mathbf{A}_i$ positions are measured, the localization application can be started. To make it more clearly, we give a case of application is the following section.

4.3.1 Case Study

The localization application depends on the purpose of the system, which can be designed for detecting, monitoring, or tracking. In this paper, the design of the localization application is a simple localization system for testing the distance error of the estimated sensor positions by the measured anchor positions. Before the phase, the anchor nodes are calibrated and $\mathbf{A}_i$'s CPC are stored on the control server. Different from acting as the transmitting node in the training phase, anchor nodes play the receiving nodes in the localization application cause to the number of anchor nodes is far less than sensor nodes and to obtain the simultaneous RSSI measurements for localization. The measured anchor positions are stored in the server.

At first, the sensor nodes periodically broadcasting signals, as shown in Figure 4.10. As the sensor node enters the field deployed with anchor nodes, the nearby anchor nodes, $\mathbf{A}_i$, receive the broadcast signals and determine the RSSI values and upload it to the server in a

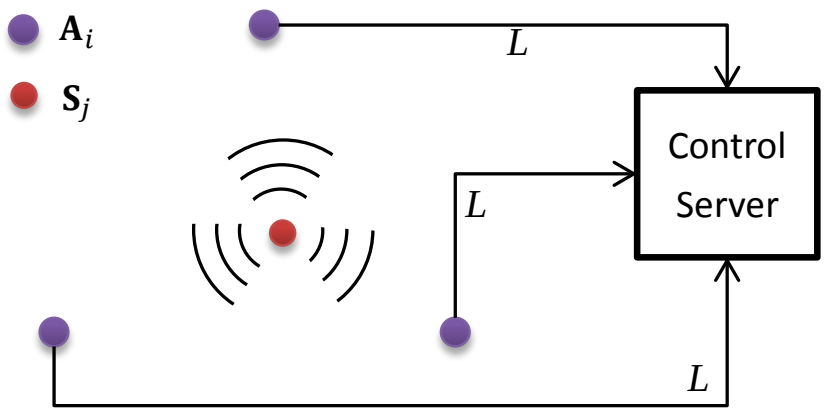

Figure 4.10: The schematic diagram of the localization phase

vector as $L = (j, r)$, where j is the identifier of $\mathbf{S}_j$, r is the RSSI measurement from $\mathbf{S}_j$. And the control server calculates the sensor position, (x_j, y_j), by trilateration algorithm with the L uploaded at the same time, where the algorithm is the same as discussed in Chapter 4.2.2. The distance error of the estimated $\mathbf{S}_j$ position is affected by the measured anchor positions. The anchor positions with more accuracy lead to more precisely sensor positioning. More, the anchor nodes' placement can also affect in the estimated sensor positions. The anchor nodes deployed with higher density can lead to more precise estimation. However, the study case is for verifying the distance error of sensor localizing in a localization system in this paper. For the purpose, anchor nodes are deployed in the lowest density in our experiments to test our approach in the worst situation.

Chapter 5

Experiments

In this chapter, we first introduce the experiment platform and its configuration, then we conduct several experiments to evaluate the calibration phase in our proposed approach. First, we introduce the hardware and environment in our experiments, and we verify the node inconsistency of the RSSI measurements by the experiment of 10 receiving nodes and 1 transmitting node. Then we estimate the CPC (calibrated propagation coefficients, discussed in Chapter 4.2.1) for each receiving node and test the distance estimation error with the CPC. At the end, we analysis the RSSI characteristics of the collected data.

5.1 Hardware and Experiment Environment

The hardware device used in the experiments is composed of a MCU (MSP430FS5438) and a RF chip (CC2500EMK). The wireless network protocol is SimpliciTI [32], which is a TI (Texas Instruments) proprietary low-power RF network protocol. The experiments take place at the hallway of second floor, Engineering Building 5, Kuang-Fu campus of NCTU. The transmitting node is set to be an anchor node, $\mathbf{A}_1$, and the 10 receiving nodes are set to be training nodes, $\mathbf{T}_k, (k = 1 \cdots 10)$. And the nodes are placed on the ground during the experiments.

5.2 Node Inconsistency

To show the node variety, we measure the RSSI values of different training nodes with the same transmitter. We collect the RSSI values of the 10 $\mathbf{T}_k$ at different distances from the anchor node, says 0.3m, 0.9m, 1.5m, 2.4m, 3.6m, and 4.8m. For each training node, 4000 RSSI values are collected at the each distance (3500 for training data and 500 for testing data). Then we calculate the average RSSI value of the 4000 collections for each device.

Table 5.1 shows the average of 3500 collected RSSI values of the 10 training nodes at distance 0.3m, 0.9m, 1.5m, 2.4m, 3.6m, and 4.8m. From the table, the RSSI values of $\mathbf{T}_5$ at 4.8m is -69.7dBm and the RSSI value of $\mathbf{T}_6$ at 3.6m is -70.2dBm. It shows that if the devices are not calibrated before distance estimation, the node variety would cause 1.2m error of distance estimation. As the result of the node variety, the training nodes should be calibrated before they can be used for localization.

Table 5.1: Mean RSSI values (dBm) of 10 training nodes

Distance	0.3m	0.9m	1.5m	2.4m	3.6m	4.8m
$\mathbf{T}_1$	-31.04	-49.37	-60.90	-66.93	-69.32	-78.95
$\mathbf{T}_2$	-29.81	-48.03	-59.03	-65.86	-68.40	-73.43
$\mathbf{T}_3$	-28.99	-46.11	-59.47	-64.77	-66.95	-78.46
$\mathbf{T}_4$	-29.94	-47.66	-59.09	-65.28	-66.63	-71.32
$\mathbf{T}_5$	-29.29	-46.21	-58.85	-64.95	-67.79	-69.60
$\mathbf{T}_6$	-32.19	-49.97	-61.27	-66.59	-70.22	-79.08
$\mathbf{T}_7$	-29.61	-47.64	-60.96	-64.31	-69.34	-79.16
$\mathbf{T}_8$	-28.82	-46.14	-58.92	-63.01	-69.93	-75.32
$\mathbf{T}_9$	-29.97	-48.56	-60.70	-62.55	-70.50	-74.13
$\mathbf{T}_{10}$	-35.13	-53.01	-60.52	-66.40	-74.07	-75.09

5.3 CPC Estimation and Test

As discussed in calibration phase in Chapter 4.2.1, the CPC (calibrated propagation coefficient) is the parameters we need for distance estimation in the localization. Following the data of Table 5.1, we calculate the CPC, a_k and b_k, for $\mathbf{T}_k$ as the method in Chapter 4.2.1. The a_k and b_k for $\mathbf{T}_k$ are shown in Table 5.2.

Table 5.2: The propagation coefficient a_k and b_k of 10 training nodes

Device	a_k	b_k
$\mathbf{T}_1$	-0.0258	-1.3307
$\mathbf{T}_2$	-0.0275	-1.3690
$\mathbf{T}_3$	-0.0250	-1.2294
$\mathbf{T}_4$	-0.0283	-1.3972
$\mathbf{T}_5$	-0.0278	-1.3581
$\mathbf{T}_6$	-0.0263	-1.3735
$\mathbf{T}_7$	-0.0250	-1.2556
$\mathbf{T}_8$	-0.0258	-1.2659
$\mathbf{T}_9$	-0.0270	-1.3527
$\mathbf{T}_{10}$	-0.0293	-1.5714

Then, 3000 testing data (500 measurements at 6 distances) are used for testing the distance estimation. The distance is measured by Equation 4.3, where a and b are replaced by a_k and b_k as:

$$d = 10^{(a_k \times r + b_k)},$$

where r is the testing data of measured RSSI value by $\mathbf{T}_k$ (500 measurements at 6 distances) and d is the estimated distance. For the comparison of non-calibrated distance estimation, we used the CPC of $\mathbf{T}_1$, a_1 and b_1, for the represent of non-calibrated propagation coefficients. For the test of each $\mathbf{T}_k$, distances are estimated through the calibrated coefficients a_k and b_k and also the non-calibrated coefficients a_1 and b_1. The distance estimation error with calibration and without calibration of each device is shown in Table 5.3. The calibration reduced 21.3% of distance

estimation error. The error is performed in meter, $|d_{est} - d_{act}|$, and percentage of the distance, $\left|\frac{d_{est} - d_{act}}{d_{act}}\right| * 100\%$. Due to the experiment result, the error of calibrated distance estimation is lower than non-calibrated estimation. To improve the accuracy of distance estimation by RSSI, the calibration is a necessary step.

Table 5.3: Average distance estimation error (in meter) at distance from 0 to 5 m

Device	error(non-calibrated)	%(non-calibrated)	error(calibrated)	%(calibrated)
$\mathbf{T}_1$	0.229 m	8.7%	0.229 m	8.7%
$\mathbf{T}_2$	0.442 m	13.6%	0.270 m	9.7%
$\mathbf{T}_3$	0.348 m	15.9%	0.345 m	13.3%
$\mathbf{T}_4$	0.537 m	16.5%	0.370 m	14.3%
$\mathbf{T}_5$	0.522 m	16.4%	0.332 m	13.1%
$\mathbf{T}_6$	0.294 m	10.0%	0.300 m	9.7%
$\mathbf{T}_7$	0.319 m	14.3%	0.302 m	12.2%
$\mathbf{T}_8$	0.257 m	13.2%	0.226 m	9.2%
$\mathbf{T}_9$	0.307 m	11.7%	0.202 m	9.2%
$\mathbf{T}_{10}$	0.294 m	15.5%	0.227 m	7.8%
Average	0.355 m	13.6%	0.2816 m	10.7%

5.4 Characteristic of RSSI

In the Log Distance Path Loss Model of signal propagation, a zero-mean Gaussian random variable with standard deviation σ, X_σ, exists and noising in the RSSI measurements. To simulate the RSSI noise in our experiments, the standard deviation σ is the parameter that needed to be defined. As the collected RSSI data in Table 5.1, the RSSI histograms reveal that the measurements fit well with the normal Gaussian distribution, shown in Figure 5.1. The standard deviation seems to increase when the RSSI value decreases. Since the measured RSSI by our devices are integers, the standard deviation σ of RSSI measurement noise is 1 dBm at 0.3 meter and 3 dBm at 4.8 meter. To find the relation between the standard deviation and the RSSI

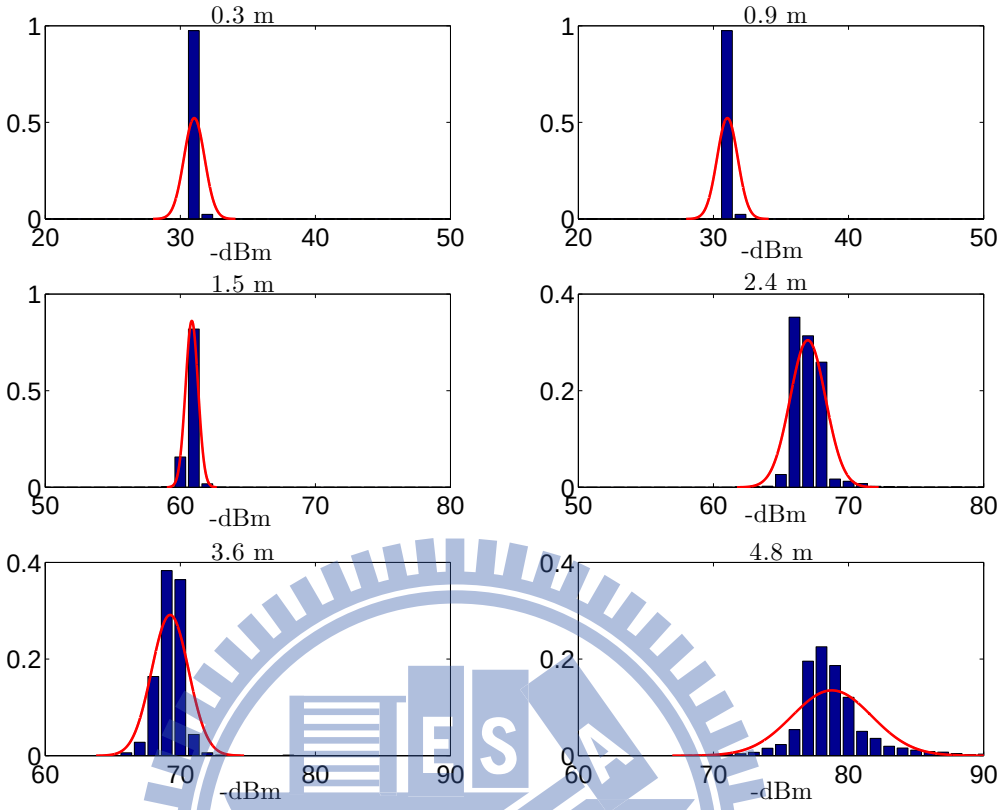

Figure 5.1: Histogram of RSSI of $\mathbf{T}_1$ at 0.3m, 0.9m, 1.5m, 2.4m, 3.6m, 4.8m

Table 5.4: Mean values and standard deviation of RSSI measurements by $\mathbf{T}_1$

Distance	0.3m	0.9m	1.5m	2.4m	3.6m	4.8m
Mean RSSI(dBm)	-31.04	-49.40	-60.85	-66.99	-69.25	-78.77
σ	0.76	0.56	0.46	1.31	1.37	2.95
$\left\lvert\frac{\sigma}{\text{RSSI}}\right\rvert$	0.0246	0.0113	0.0076	0.0196	0.0198	0.0375

value, the ratio of $\left\lvert\frac{\sigma}{\text{RSSI}}\right\rvert$ from $\mathbf{T}_1$ collected data are listed in Table 5.4. In our simulation, we choose the largest $\left\lvert\frac{\sigma}{\text{RSSI}}\right\rvert$ ratio, 0.0375, as the noise parameter of Gaussian variable in RSSI measurement. The standard deviation σ in the Gaussian variable is set to be $|\text{RSSI}|$*(0.0375), where the σ increases when the RSSI decreases.

Chapter 6

Simulation & Comparison

In this chapter, we verify the correctness of our proposed approach on the anchor nodes locating in the training phase and the sensor nodes locating in the localization phase. Due to the serious signal interferences in the campus buildings (Figure 3.2 shows the interference of second floor Engineering Building 5, Kuang-Fu campus of NCTU), we conduct the experiments with Matlab for the verification. The real signal propagation data from the experiments in the above chapter is involved to make our simulation closer to actual situation.

6.1 Setup

To justify that the proposed algorithm is practical, we simulate the algorithm via Matlab (The MathWorks, USA) Version 7.10.0.499 (R2010a). The simulation area is 15m $\times$ 13m, which simulates the second floor, Engineering Building 5, Kuang-Fu campus of NCTU. The anchor nodes are placed in the lowest density, which ensures everywhere has 3 anchor coverage. For the device and the protocol we used in Chapter 5, the RSSI value fluctuated seriously over 5 meters. Therefore, we assume the maximum transmitting range of the wireless signal is 5 meters. Due to the transmitting range, we deployed 23 anchor nodes($\mathbf{A}_i, I = 23$) in the area, where the distance between $\mathbf{A}_i$ is 3.75 meters. The environment is shown in Figure 6.1, where black circles are the location of anchor nodes. If the other protocol is substitute in, such as Bluetooth or Zigbee, the transmitting range can be set to 10 meters or longer and the less anchor nodes can be used in the same area. In the simulation, all the anchor nodes and training nodes are assumed to be placed in two parallel plane: anchor nodes are placed at the ceiling, training

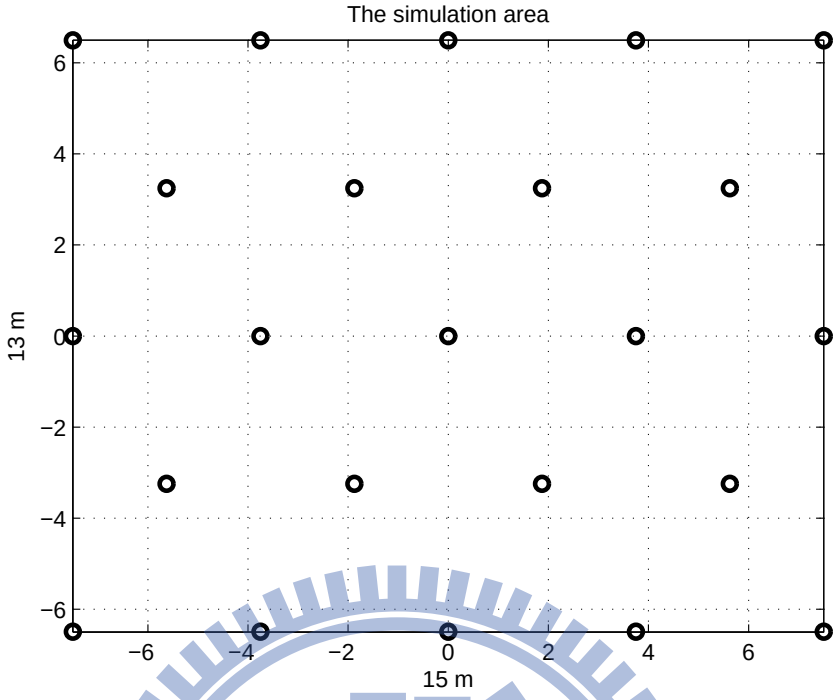

Figure 6.1: The simulation area

nodes and sensor nodes are hung in front of the chest of users. The height between the ceiling and the chest of users are assumed to be 1.5 meter (all users are at the same height).

6.2 Design

To verify our approach, four experiments are designed in this paper. Three experiments are designed for the testing of training phase and finding the appropriate number of two parameters in the training phase. And one experiment is designed for the testing of localization phase.

Exp#1: Removing the starting restrictions

The objective of Exp#1 is to verify that the restrictions of starting direction and starting position can be removed in our algorithm. Two conditions of training phase are designed: one is that all training nodes are started with restrictions, and the other is without restrictions. To

compare the distance error of estimated anchor positions of two conditions, the threshold of collected RSSI values is set to the same value. The distance error is compared at different settings of the training node numbers.

Exp#2: Finding the proper setting of K

To determine the number of training nodes used in the training phase, we design the experiment to measuring anchor positions with different numbers of K. Theoretically, the distance error decreases as K increase since the noise of RSSI measurements and navigation measurements are averaged. However, the larger K means the more cost due to more devices are used. Therefore, there is a need to find an appropriate K to balance the cost and accuracy. The range of K varies from 1 to 20. And we list the distance error of estimated anchor positions with K for analysing. The threshold of collected RSSI value, MRC, is set to the same value.

Exp#3: Finding the proper setting of MRC

To determine the MRC in the training phase, we design the experiment to measuring anchor positions with different MRC. It is used to determine when a training of a training node is done: for all n_i are over MRC, where n_i is the number of measured RSSI values of each anchor nodes, $\mathbf{A}_i$ $(i = 1, 2, \cdots, I)$. Theoretically, the distance error decreases as MRC increases since to the averaging of the noise. But the larger MRC means the longer period of the training phase, which consumes more power. Therefore, there is a need to find an appropriate number of MRC. Since the trilateration needs at least three measurements to localize the target, MRC is set to varying from 3 to 8 in the experiment.

Exp#4: Locating sensor nodes

The objective of Exp#4 is to evaluate the localization error by using measured anchor positions. First, the anchor positions are measured through the training phase with the appropriate settings determined in Exp#2 (K) and Exp#3 (MRC) and training nodes start from different directions and positions. After the anchor positions are measured, the sensor nodes, $\mathbf{S}_j$, are randomly set in the area. The positions of $\mathbf{S}_j$ are measuring through the localization phase. For comparison, the localization with actual anchor positions, which are manually configured, is also tested in this experiment.

6.3 Noise Source

Before we start our simulation, there are two sources of noise that may influence the accuracy of the measured anchor positions in our approach:

- Navigation system: the position estimation error of the navigation.
- RSSI measurement: the physical interference on path loss of wireless signal.

To make our experiment closer to actual situation, the noises must be inducted into our experiments.

6.3.1 Noise of Navigation System

To simulate the noise of the navigation system, the design of Hansson [20] is inducted into our experiments. The estimating error model defined by Hansson is shown in Equation 3.1. In the Equation 3.1, there are two coefficients need to be defined in our experiments. The coefficient t is the time since the start of the navigation in seconds. It is determined by the

total walking length and the walking speed. The total walking length is calculated from the message sent by training node, and the walking speed is set as 1.4 m/s, according to the studies of [33][34]. The coefficient d is the estimated distance to the start point in meters. It is determined by the distance from current uploading position of training node to the origin in the local coordinates (the start point of training node is defined as the origin in local coordinates). Therefore, when the current estimated position of navigation system is $\mathbb{C}_k(x, y)$ at $\mathbb{C}_k$, the error of navigation system is calculated as

$$e = -0.2398 + 0.0152 \times \frac{\text{Total walking length}}{1.4} + 0.1081\sqrt{x^2 + y^2}.$$

6.3.2 Noise of RSSI Measurement

To simulate the noise of RSSI measurements, the Gaussian random variable, X_σ, in the Equation 4.1 is defined in the simulation. The mean of the Gaussian random variable is defined to be zero, and the standard deviation, σ, is defined to increase with the value of $|\text{RSSI}|$. The equation of σ value is

$$\sigma = 0.0375 \times |\text{RSSI}|,$$

where the value of 0.0375 is the largest ratio of $\left|\frac{\sigma}{\text{RSSI}}\right|$ from the real data collected in the experiment in Chapter 5.

6.4 Simulation Results

The four designed experiments are performed with the estimated parameters in the above chapter. We assume that all training nodes $\mathbf{T}_k$ and anchor nodes $\mathbf{A}_i$ are calibrated with CPC before they are used. The results of each experiment are in the followings.

6.4.1 The Result of Exp#1

The Exp#1 examines the removing of the constraints of the start heading and location in the navigation system. Without the same start heading and location, each training node builds up a local coordinate system $\mathbb{C}_k$ and measure the position at $\mathbb{C}_k$ by navigation system. To examine that our approach can integrate the local coordinates of training node and measure the anchor positions correctly, the distance error of anchor positions measuring without restrictions are compared with the error of anchor positions measuring with restrictions. The comparison is done when the number of training nodes goes from 1 to 8. 1000 times of testing are done and the results of the two situations are shown in Figure 6.2. As in the figure, the error of

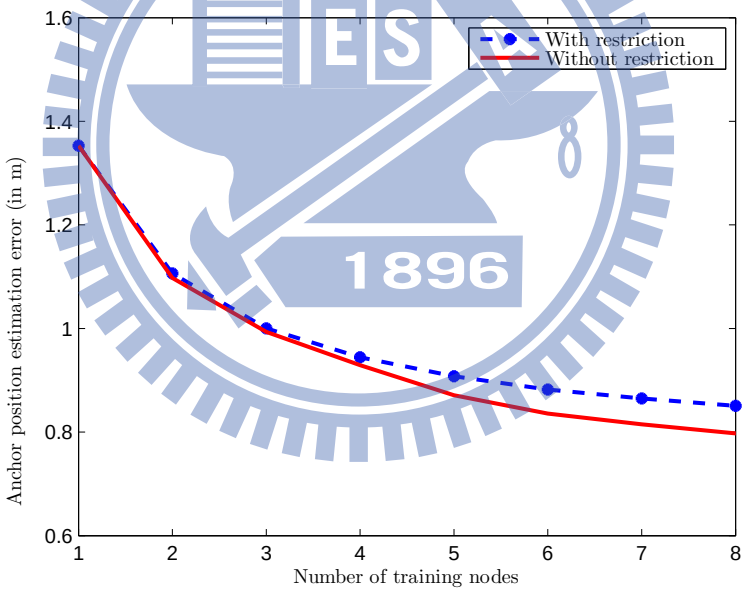

Figure 6.2: The result of Exp#1

training with different starting conditions is lower than the error of training with the same start condition. It's because the estimated training path error is averaged by starting at different location. Accordingly, the restrictions of the starting direction and position are removed in our approach.

6.4.2 The Result of Exp#2

The Exp#2 finds the appropriate number of training nodes, K, using in the training phase. In the experiment, 1 to 20 training nodes (K = 1, 2,$\cdots$, 20) are used to measure the anchor positions. 1000 times of tests are performed and the distance error of anchor positions by different numbers of K is shown in Figure 6.3. We can see that the distance error of using only

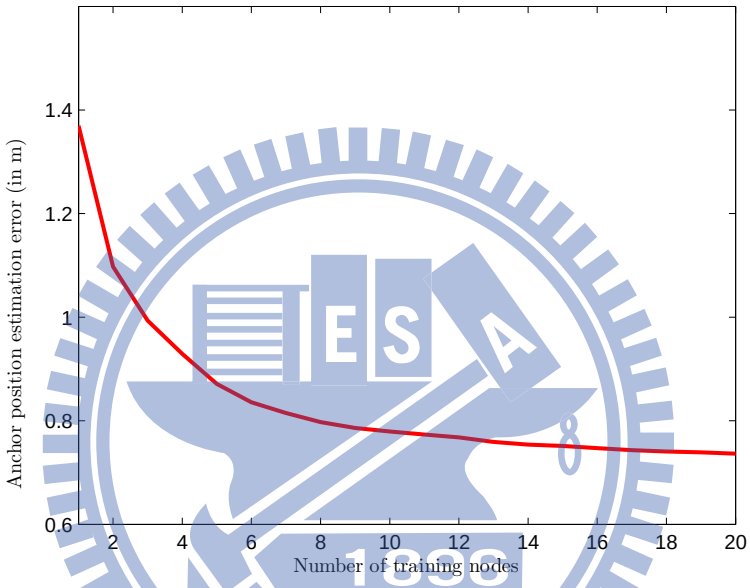

Figure 6.3: Simulation of reverse localization with different numbers of training nodes

one training node is about 1.37 meters. When one training node is added in the training phase, the distance error decrease fast when using more training nodes until using 8 training nodes, where the improve percentage are more than 2% as shown in Table 6.1. When the number of training nodes is over 8, the localization error decrease slowly (less than 2%). Therefore, we conclude that 8 training nodes are proper for training phase, and the expected localization error is below 0.8 meters.

Table 6.1: Improve percentage of adding 1 training node at each K

K	1	2	3	4	5	6	7	8	9
Distance error (m)	1.37	1.10	1.00	0.93	0.87	0.83	0.80	0.78	0.77
Improvement	-	19.7%	9.1%	7.0%	6.5%	4.6%	3.6%	2.5%	$\leq 2\%$

6.4.3 The Result of Exp#3

The Exp#3 determines the proper setting of MRC for the training phase. In the experiment, MRC are set from 3 to 8 in the training phase for measuring anchor positions. For the tests, 8 training nodes ($K = 8$) are used since the result of Exp#2 shows that it is the appropriate number for the training phase. 1000 times of testing are performed and the distance error of anchor positions by the different number of MRC is listed in Table 6.2. The distance error is 1.1228 meters when MRC is set to 3, which is too large for using in the localization phase. When MRC is set to 4, the distance error is less than 0.8 meters. For the larger MRC, the distance error decreases but with little improvement, where the distance errors are all between 0.7 and 0.8 meters. Therefore, we conclude that the MRC = 4 is the appropriate setting for the training phase. Which means a training node needs to receive at least four RSSI measurements from each anchor nodes.

Table 6.2: Average error of measuring anchor nodes position by different MRC

MRC	3	4	5	6	7	8
Distance error	1.1228 m	0.7877 m	0.7827 m	0.7754 m	0.7413 m	0.7378 m

6.4.4 The Result of Exp#4

The Exp#4 evaluates the performance of the sensor nodes locating in the localization phase using measured anchor positions by our approach. The settings for training phase are K = 8

and MRC = 4, as the result of Exp#2 and Exp#3. After the training phase, the measured anchor positions are used in the localization phase. And as the comparison, the localization phase is also performed with actual anchor positions. For each test, 100 sensor nodes are randomly placed in the 15m×13m field. And 1000 tests are performed with the simulation. First, we examine the result of the measured anchor positions in training phase. The distance error range between the measured anchor positions and actual anchor positions of the 1000 tests is from 0.544 to 1.563 meters, where the mean is 0.78 meters. Then the result of sensor nodes locating using measured anchor positions and using actual anchor positions are shown in Table 6.3. The distance error with actual anchor positions is 0.67 meter as the error with measured anchor positions is 0.732 meter. The localization using measured anchor positions by our approach increases 0.062 meter in localization error, which only increases 9.25% of error when using actual anchor positions.

Table 6.3: Distance error of sensor nodes locating in the localization phase

Localization with	Distance error	Standard deviation
Actual anchor positions	0.670 m	0.042 m
Measured anchor positions	0.732 m	0.074 m

6.5 Comparison

In this section, we give the comparison of our proposed approach and other methods on the RSSI measurement, additional hardware and restrictions, and power consumption.

RSSI measurements

First, we discuss the RSSI measurement in our proposed approach and other three methods. In our approach, the CPC (calibrated propagation coefficient) of each node that requires to measure RSSI value are given to the control server to improve the distance estimation. As the result in Chapter5, the error of distance estimation with calibration is 23.5% less than the estimation without calibration. In Jones' method, since there is only one special vehicle for collecting RSSI values, there is no need of calibration. The propagation model can be defined just fit the special vehicle. In Chun's and Hansson's methods, there are several smartphones using to collecting RSSI values but without calibration. As the result of node inconsistency between devices, the distance estimation by RSSI value is less accurate than the estimation with calibration.

Additional Hardware and Restriction

To compare with other approaches, we list the usage of additional hardware and the restrictions in each approach, as shown in Table 6.4. Both Jones' and Chun's methods required GPS module, which is the most undesired component in WSN, to record the position of the device that used for locating anchor nodes. The GPS module is expensive and power-consuming and takes seconds to obtain the GPS coordinate, which is not suitable for the low-cost, low-power sensors in WSN. Furthermore, since the GPS functions poorly indoors, it is not appropriate to be used in the indoor applications.

Hansson's and our proposed approaches remove the usage of GPS module and replace it with small sensors to build an inertial navigation system. Benefit from the recent advances of MEMS IC technology, the sensors such as accelerometer and gyroscope are manufactured small and light that can be equipped on sensor nodes with low power-consuming. In the Hans-

Table 6.4: Comparison of the approaches

Approach			Jones'	Chun's	Hansson's	Proposed
Additional hardware	GPS module		◯	◯	×	×
	Sensors	Accelerometer	×	×	◯	◯
		Gyroscope	×	×	◯	◯
		Magnetometer	×	×	◯	×
Restrictions	Start direction		N/A	N/A	restricted	non-restricted
	Start position		N/A	N/A	restricted	non-restricted

◯: Required
× : Not required

son's approach, the magnetometer is used to aid the orientation tracker. But the magnetometer measurement is not reliable enough to used, they limit the usage of the magnetometer in the orientation estimation. In our proposed approach, the magnetometer is removed from our navigation system since the unreliable measurement and the magnetic disturbance in the indoor environment. In Hansson's approach, the navigation systems in each smartphone record position in a global coordinate system and they collect all data from smartphones to compute the position. For that, they restrict the start direction and position of the smartphones, which leads to estimate positions are always with more error in the area apart from the start position than the area near the start position. Consequently, we remove the restrictions and replace local coordinate systems to the navigation systems on each training node. And by the training of each training node, the positions of anchor nodes are first computed at local coordinate systems. Then we integrate anchor positions in all local coordinate systems into a global coordinate systems. Thus, the errors of estimated positions are averaged over the test area and the users can start the training with no restrictions.

Power Consumption

To compare the power consumption between approaches, we first list the power consumption of GPS module, accelerometer and gyroscope. As shown in the Table 6.5, the power

Table 6.5: Power consumption of GPS, accelerometer, and gyroscope

Modules	Power (mW)
GPS (u-blox ANTARIS 4 in Openmoko) [35]	143.1
Accelerometer (ADXL335) [36]	1.24
Gyroscope (LPR530AL + LY530ALH) [36]	40.59

consumption of GPS is 143.1 mW [35], where the GPS module is *u-blox ANTARIS 4* in the Openmoko Neo Freerunner (reversion A6) mobile phone. The power consumption of an inertial navigation system using accelerometer and gyroscope is 41.83 mW [36], where the accelerometer module is *ADXL335* (triple-axis) and gyroscope modules are *LPR530AL* (pitch and roll gyro) and *LY530ALH* (yaw gyro).

In our simulation, the average training time of a training node in the training phase is 60 seconds when MRC is set to 4. Assume that the GPS module and the accelerometer and gyroscope modules are all power on during the training in each approach (GPS used in Jones' and Chun's methods and accelerometer and gyroscope used in Hansson's and our proposed approaches). The total energy consumption of Jones' and Chun's methods on the GPS module are 8.58 Joule, where the Hansson's method and our proposed approach are 2.5 Joule. The energy consumption of accelerometer and gyroscope is 70% less than GPS module.

6.6 Summary

In this chapter, we demonstrate the proposed approach that can be applied to locate anchor nodes in WSN. In the experiments, we evaluate the appropriate setting of K and MRC and then

used the setting to locate anchor nodes. Then we verified that the measured anchor positions can be used to locate sensor nodes in the WSN localization applications. In conclusion, our proposed approach provides a way to locate anchor nodes with fewer extra components than other methods. And the localization error of sensor nodes with anchor positions measured by our approach doesn't increase much than the actual anchor positions.

Chapter 7

Conclusion and Future Work

In this research, taking Hansson's method as a basis, we proposed a reverse localization approach in WSN to locate anchor nodes. Our approach locates anchor nodes based on RSSI values. An inertial navigation system is conducted with gyroscope and accelerometer to avoid using GPS devices. Also, the coordinates transformation with Procrustes analysis is involved for the training without restrictions on start direction and position. To demonstrate there are no restrictions in our proposed approach, we design an experiment to test the anchor node locating. The experiment verifies that our approach locates anchor node with the performance as the approach with restrictions, such that the restrictions are unnecessary in our approach. To demonstrate the proposed approach can be applied to locate sensor nodes in the applications, we design an experiment to test the sensor node locating based on the measured anchor positions. The experiment demonstrates that the measured anchor position by our approach is able to locate sensor nodes.

In the next step, we will improve the algorithm of position computing of the trilateration. Based on the proposed approach, the error of estimated position on the navigation system can be involved into the position computing, such as the weighting of the RSSI measurements. The proposed approach is based on the basic trilateration algorithm and the optimizing method could be added in the future.

References

[1] I. Akyildiz, W. Su, Y. Sankarasubramaniam, and E. Cayirci, "Wireless sensor networks: a survey," *Computer Networks*, vol. 38, no. 4, pp. 393 – 422, 2002. [Online]. Available: http://www.sciencedirect.com/science/article/pii/S1389128601003024

[2] C.-Y. Chong and S. Kumar, "Sensor networks: evolution, opportunities, and challenges," *Proceedings of the IEEE*, vol. 91, no. 8, pp. 1247 – 1256, aug. 2003.

[3] M. Bal, M. Liu, W. Shen, and H. Ghenniwa, "Localization in cooperative Wireless Sensor Networks: A review," in *Computer Supported Cooperative Work in Design, 2009. CSCWD 2009. 13th International Conference on*, april 2009, pp. 438 –443.

[4] N. B. Priyantha, H. Balakrishnan, E. Demaine, and S. Teller, "Anchor-free distributed localization in sensor networks," *Science*, vol. 8, no. SenSys, pp. 340–341, 2003. [Online]. Available: http://en.scientificcommons.org/43019921

[5] B. Parkinson and J. Spilker, *Global positioning system: theory and applications*, ser. Progress in astronautics and aeronautics. American Institute of Aeronautics and Astronautics, Inc., 1997. [Online]. Available: http://books.google.com.tw/books?id=lvI1a5J_4ewC

[6] P. Enge and P. Misra, "Special Issue on Global Positioning System," *Proceedings of the IEEE*, vol. 87, no. 1, pp. 3 –15, jan. 1999.

[7] A. Joshi, I. VishnuKanth, N. Samdaria, S. Bagla, and P. Ranjan, "GPS-less animal tracking system," in *Wireless Communication and Sensor Networks, 2008. WCSN 2008. Fourth International Conference on*, dec. 2008, pp. 120 –125.

[8] N. Bulusu, J. Heidemann, and D. Estrin, "GPS-less low-cost outdoor localization for very small devices," *Personal Communications, IEEE*, vol. 7, no. 5, pp. 28 –34, oct 2000.

[9] S. Capkun, M. Hamdi, and J. Hubaux, "GPS-Free Positioning in Mobile ad-hoc Networks," in *Proceedings of the 34th Annual Hawaii International Conference on System Sciences (HICSS-34)-Volume 9 - Volume 9*, ser. HICSS '01. Washington, DC, USA: IEEE Computer Society, 2001, pp. 9008–. [Online]. Available: http://dl.acm.org/citation.cfm?id=820738.820818

[10] D. Niculescu and B. Nath, "Ad hoc positioning system (APS)," in *Global Telecommunications Conference, 2001. GLOBECOM '01. IEEE*, vol. 5, 2001, pp. 2926 –2931 vol.5.

[11] A. Nasipuri and K. Li, "A directionality based location discovery scheme for wireless sensor networks," in *Proceedings of the 1st ACM international workshop on Wireless sensor networks and applications*, ser. WSNA '02. New York, NY, USA: ACM, 2002, pp. 105–111. [Online]. Available: http://doi.acm.org/10.1145/570738.570754

[12] E.-E.-L. Lau and W.-Y. Chung, "Enhanced RSSI-Based Real-Time User Location Tracking System for Indoor and Outdoor Environments," in *Proceedings of the 2007 International Conference on Convergence Information Technology*, ser. ICCIT '07. Washington, DC, USA: IEEE Computer Society, 2007, pp. 1213–1218. [Online]. Available: http://dx.doi.org/10.1109/ICCIT.2007.199

[13] Z. Fang, Z. Zhao, D. Geng, Y. Xuan, L. Du, and X. Cui, "RSSI variability characterization and calibration method in wireless sensor network," in *Information and Automation (ICIA), 2010 IEEE International Conference on*, june 2010, pp. 1532 –1537.

[14] T. Rappaport, *Wireless Communications: Principles and Practice*, 2nd ed. Upper Saddle River, NJ, USA: Prentice Hall PTR, 2001.

[15] K. Aamodt, ”CC2431 Location Engine,” Chipcon Products from Texas Instruments, Application Note AN042 (Rev. 1.0), SWRA095, Tech. Rep., 2008.

[16] S. Zickler and M. Veloso, ”RSS-based relative localization and tethering for moving robots in unknown environments,” in *Robotics and Automation (ICRA), 2010 IEEE International Conference on*, may 2010, pp. 5466 –5471.

[17] S. Simic and S. S. Sastry, ”Distributed localization in wireless ad hoc networks,” EECS Department, University of California, Berkeley, Tech. Rep. UCB/ERL M02/26, 2002. [Online]. Available: http://www.eecs.berkeley.edu/Pubs/TechRpts/2002/4010.html

[18] V. Ramadurai and M. L. Sichitiu, ”Localization in wireless sensor networks : A probabilistic approach,” *System*, vol. 02, no. 05, p. 275–281, 2003. [Online]. Available: http://ieeexplore.ieee.org/xpls/abs_all.jsp?arnumber=5946723

[19] O. J. Woodman, ”An introduction to inertial navigation,” University of Cambridge, Computer Laboratory, Tech. Rep. UCAM-CL-TR-696, Aug. 2007. [Online]. Available: http://www.cl.cam.ac.uk/techreports/UCAM-CL-TR-696.pdf

[20] A. Hansson and L. Tufvesson, ”Using Sensor Equipped Smartphones to Localize WiFi Access Points,” Master’s thesis, Department of Automatic Control, Lund University, 2011. [Online]. Available: http://lup.lub.lu.se/luur/download?func=downloadFile&recordOId=2174317&fileOId=2174332

[21] J. Gower and G. Dijksterhuis, *Procrustes problems*, ser. Oxford statistical science series. Oxford University Press, 2004. [Online]. Available: http://books.google.com.tw/books?id=ukeWSQx0LoAC

[22] A. Ross, ”Procrustes Analysis,” Department of Computer Science and Engineering

University of South Carolina, SC 29208, Tech. Rep., 2004. [Online]. Available: http://www.cse.sc.edu/~songwang/CourseProj/proj2004/ross/ross.pdf

[23] C. Goodall, "Procrustes methods in the statistical analysis of shape," *Journal of the Royal Statistical Society. Series B (Methodological)*, vol. 53, no. 2, pp. pp. 285–339, 1991. [Online]. Available: http://www.jstor.org/stable/2345744

[24] B. Tatham, "Anchor node placement for localization in wireless sensor networks," Master's thesis, Department of Systems and Computer Engineering Carleton University, January 2011.

[25] Q.-L. Du, Z.-H. Qian, H. Jiang, and S.-X. Wang, "Localization of Anchor Nodes for Wireless Sensor Networks," in *New Technologies, Mobility and Security, 2008. NTMS '08.*, nov. 2008, pp. 1 –5.

[26] Russel Kipp Jones (Roswell, GA, US), Farshid Alizadeh-shabdiz (Wayland, MA, US), Edward James Morgan (Needham, MA, US), Michael George Shean (Boston, MA, US), "Server for updating location beacon database," Patent 8 031 657, October, 2011. [Online]. Available: http://www.freepatentsonline.com/8031657.html

[27] S.-M. Chun, S.-M. Lee, J.-W. Nah, J.-H. Choi, and J.-T. Park, "Localization of Wi-Fi Access Point using smartphone's GPS information," in *Mobile and Wireless Networking (iCOST), 2011 International Conference on Selected Topics in*, oct. 2011, pp. 121 –126.

[28] T. Scott, K. Wu, and D. Hoffman, "Radio propagation patterns in wireless sensor networks: new experimental results," in *Proceedings of the 2006 international conference on Wireless communications and mobile computing*, ser. IWCMC '06. New York, NY, USA: ACM, 2006, pp. 857–862. [Online]. Available: http://doi.acm.org/10.1145/1143549.1143721

[29] S. Biaz, J. Yiming, B. Qi, and S. Wu, "Dynamic signal strength estimates for indoor wireless communications," in *Wireless Communications, Networking and Mobile Computing, 2005. Proceedings. 2005 International Conference on*, vol. 1, sept. 2005, pp. 602 – 605.

[30] D. G. Kendall, "A survey of the statistical theory of shape," *Statistical Science*, vol. 4, no. 2, pp. 87–99, 1989.

[31] "Procrustes analysis." [Online]. Available: http://www.mathworks.com/help/toolbox/stats/procrustes.html

[32] "SimpliciTI Overview (Rev. B)," Texas Instruments, Tech. Rep., 2008. [Online]. Available: http://www.ti.com/lit/ml/swru130b/swru130b.pdf

[33] R. C. Browning, E. A. Baker, J. A. Herron, and R. Kram, "Effects of obesity and sex on the energetic cost and preferred speed of walking," *Journal of Applied Physiology*, vol. 100, no. 2, pp. 390–398, 2006. [Online]. Available: http://jap.physiology.org/content/100/2/390.abstract

[34] R. V. Levine and A. Norenzayan, "The Pace of Life in 31 Countries," *Journal of Cross-Cultural Psychology*, vol. 30, no. 2, pp. 178–205, 1999. [Online]. Available: http://jcc.sagepub.com/content/30/2/178.abstract

[35] A. Carroll and G. Heiser, "An analysis of power consumption in a smartphone," in *Proceedings of the 2010 USENIX Annual Technical Conference*, Boston, MA, USA, Jun 2010, pp. 1–12.

[36] C. Gan, "Design of inertial tracking system for laparoscopic instrument trajectory analysis," 2010. [Online]. Available: http://digitalcommons.mcmaster.ca/ee4bi6/35